

The transverse momentum distribution of hadrons within jets

Zhong-Bo Kang^{a,b,c}, Xiaohui Liu^d, Felix Ringer^e and Hongxi Xing^{f,g}

^a*Department of Physics and Astronomy, University of California, Los Angeles, California 90095, USA*

^b*Mani L. Bhaumik Institute for Theoretical Physics, University of California, Los Angeles, California 90095, USA*

^c*Theoretical Division, Los Alamos National Laboratory, Los Alamos, New Mexico 87545, USA*

^d*Center of Advanced Quantum Studies, Department of Physics, Beijing Normal University, Beijing 100875, China*

^e*Nuclear Science Division, Lawrence Berkeley National Laboratory, Berkeley, California 94720, USA*

^f*Department of Physics and Astronomy, Northwestern University, Evanston, Illinois 60208, USA*

^g*High Energy Physics Division, Argonne National Laboratory, Argonne, Illinois 60439, USA*

E-mail: zkang@physics.ucla.edu, xiliu@bnu.edu.cn, fmringer@lbl.gov,
hxing@northwestern.edu

ABSTRACT: We study the transverse momentum distribution of hadrons within jets, where the transverse momentum is defined with respect to the standard jet axis. We consider the case where the jet substructure measurement is performed for an inclusive jet sample $pp \rightarrow \text{jet} + X$. We demonstrate that this observable provides new opportunities to study transverse momentum dependent fragmentation functions (TMDFFs) which are currently poorly constrained from data, especially for gluons. The factorization of the cross section is obtained within Soft Collinear Effective Theory (SCET), and we show that the relevant TMDFFs are the same as for the more traditional processes semi-inclusive deep inelastic scattering (SIDIS) and electron-positron annihilation. Different than in SIDIS, the observable for the in-jet fragmentation does not depend on TMD parton distribution functions which allows for a cleaner and more direct probe of TMDFFs. We present numerical results and compare to available data from the LHC.

Contents

1	Introduction	1
2	The semi-inclusive TMD fragmenting jet function	3
2.1	Definition	3
2.2	Factorization theorem	4
2.3	Hard functions	5
2.4	TMD fragmentation functions	7
2.4.1	Perturbative results	7
2.4.2	Renormalization	8
2.4.3	Matching onto collinear FFs	9
2.5	Soft functions	10
2.6	Solution of the evolution equations and resummation	11
2.6.1	Proper TMD definitions	12
2.6.2	Hard matching functions	13
2.6.3	Relation between in-jet and standard TMDFFs	14
2.6.4	Solution for the siTMDFJFs	15
2.7	Final expression for the siTMDFJFs	16
3	Phenomenology for $pp \rightarrow (\text{jet } h)X$	18
4	Conclusions	22

1 Introduction

In recent years, studies of jets and their internal structure have played increasingly important roles in testing the fundamental properties of Quantum Chromodynamics (QCD), and in searching for new physics beyond the Standard Model [1, 2]. This is the case in particular in the era of the Large Hadron Collider (LHC), where collimated jets of hadrons are abundantly produced.

In this paper we study the transverse momentum distribution of hadrons h within fully reconstructed jets in pp collisions, $pp \rightarrow (\text{jet } h)X$, as illustrated in Fig. 1. Specifically we study the ratio

$$F(z_h, \mathbf{j}_\perp; \eta, p_T, R) = \frac{d\sigma^{pp \rightarrow (\text{jet } h)X}}{dp_T d\eta dz_h d^2\mathbf{j}_\perp} \bigg/ \frac{d\sigma^{pp \rightarrow \text{jet } X}}{dp_T d\eta}, \quad (1.1)$$

where the numerator and denominator are the differential jet cross sections with and without the reconstruction of the hadron h inside the jet. The variables η , p_T and R are the rapidity, the transverse momentum and the jet size parameter of the reconstructed jet measured in

the center-of-mass (CM) frame in pp collisions. The large light-cone momentum fraction of the jet carried by the hadron h is denoted by z_h and \mathbf{j}_\perp is the transverse momentum of the hadron with respect to the standard jet axis. Throughout this paper, bold letters represent two-dimensional transverse momentum vectors, whereas the magnitude of these vectors is referred to as, for example, $j_\perp = |\mathbf{j}_\perp|$. This observable has been measured at the LHC in pp collisions for a wide range of jet transverse momenta p_T [3]. In addition, it has been measured in both unpolarized pp and transversely polarized $p^\uparrow p$ collisions at the Relativistic Heavy Ion Collider (RHIC) [4–6]. It was proposed in [7] that the latter case can be used to probe azimuthal spin correlations in the fragmentation process, in particular, the so-called Collins function [8].

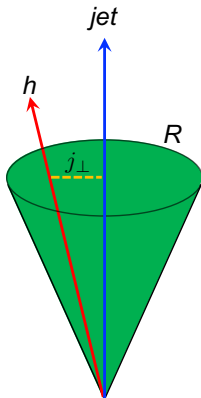


Figure 1. The Distribution of hadrons inside a fully reconstructed jet. Here, j_\perp is the transverse momentum of hadrons with respect to the standard jet axis, and R is the jet radius.

In this work, we develop the theoretical framework to study the above observable $F(z_h, \mathbf{j}_\perp; \eta, p_T, R)$. We consider the case where the jet substructure measurement is performed for an inclusive jet sample $pp \rightarrow \text{jet} + X$, different than the study in [9] where an exclusive jet sample was studied in the context of heavy quarkonium production. As the experimental measurements [3] were performed for inclusive jet samples, our approach facilitates a direct comparison with the experimental data. In particular, we concentrate on the region of the hadron transverse momentum where $j_\perp \ll p_T R$. Here, j_\perp is defined with respect to the standard jet axis, rather than a recoil-free axis, specifically the winner-take-all jet axis as discussed in [10]. While a recoil-free axis can be advantageous for various applications for collider physics, it turns out that there is only a direct relation to the standard transverse momentum dependent fragmentation functions (TMDFFs) when the standard jet axis is used. The standard TMDFFs are also probed in the traditional processes semi-inclusive deep inelastic scattering (SIDIS) and back-to-back hadron pair production in electron-positron annihilation.

Following earlier work on the longitudinal momentum distribution of hadrons inside jets [11–16], we can write down the factorized form of the cross section in pp collisions as

follows (for more details, see Eq. (3.1) below)

$$\frac{d\sigma^{pp \rightarrow (\text{jet } h)X}}{dp_T d\eta dz_h d^2\mathbf{j}_\perp} = \sum_{a,b,c} f_a(x_a, \mu) \otimes f_b(x_b, \mu) \otimes H_{ab}^c(x_a, x_b, \eta, p_T/z, \mu) \otimes \mathcal{G}_c^h(z, z_h, \omega_J R, \mathbf{j}_\perp, \mu). \quad (1.2)$$

Here, $f_{a,b}$ denote the parton distribution functions (PDFs) in the proton with the corresponding momentum fraction x_a and x_b , respectively. The hard functions H_{ab}^c describe the production of an energetic parton c in the hard-scattering event. In addition, the functions $\mathcal{G}_c^h(z, z_h, \omega_J R, \mathbf{j}_\perp, \mu)$ are the semi-inclusive TMD fragmenting jet functions (siTMDFJFs) which we describes the production of a jet in the final state with the observed hadron inside. We define this new function in Sec. 2 below. We further demonstrate that the siTMDFJFs can be refactorized in terms of hard matching functions, soft functions, and the transverse momentum dependent fragmentation functions. It is evident that the in-jet fragmentation of hadrons considered in this work provides a very sensitive probe especially for the gluon TMDFF which is so far only poorly constrained by the traditional processes.

The remainder of this paper is organized as follows. In Sec. 2, we provide operator definitions for the siTMDFJFs \mathcal{G}_c^h , which is the essential component in describing the hadron transverse momentum distribution inside jets. We derive a factorization formalism for siTMDFJFs in terms of hard functions, soft functions and the TMDFFs. We calculate all these relevant functions in the factorized expression to next-to-leading order (NLO) and derive their renormalization group equations. We solve the resulting renormalization group (RG) equations in order to resum all the relevant large logarithms. In Sec. 3, we provide a first numerical estimate for the hadron transverse momentum distribution inside jets for LHC kinematics, and we compare with experimental results. We summarize our paper and provide further discussions in Sec. 4.

2 The semi-inclusive TMD fragmenting jet function

In this section, we introduce the definition of the semi-inclusive TMD fragmenting jet functions $\mathcal{G}_c^h(z, z_h, \omega_J R, \mathbf{j}_\perp, \mu)$, which are the relevant new ingredients in order to describe the hadron transverse momentum distribution within jets produced in pp collisions. The siTMDFJFs describe the fragmentation of a hadron h inside a jet that is initiated by a parton c . We first provide their operator definitions, and we then derive the factorization formalism in terms of hard functions, soft functions and TMDFFs. We derive the relevant RG equations and their solutions. In addition, we work out the relation to standard TMDFFs probed in SIDIS and electron-positron annihilation.

2.1 Definition

Following the convention for the definition of the semi-inclusive fragmenting jet function in [16], the siTMDFJFs are defined for quark and gluon jets as follows

$$\mathcal{G}_q^h(z, z_h, \omega_J R, \mathbf{j}_\perp, \mu) = \frac{z}{2N_c} \delta\left(z_h - \frac{\omega_h}{\omega_J}\right) \text{Tr} \left[\frac{\not{n}}{2} \langle 0 | \delta(\omega - \bar{n} \cdot \mathcal{P}) \delta^2(\mathcal{P}_\perp - \mathbf{j}_\perp) \chi_n(0) | (Jh)X \rangle \right]$$

$$\times \langle (Jh)X | \bar{\chi}_n(0) | 0 \rangle \Big], \quad (2.1a)$$

$$\begin{aligned} \mathcal{G}_g^h(z, z_h, \omega_J R, \mathbf{j}_\perp, \mu) = & - \frac{z \omega}{(d-2)(N_c^2 - 1)} \delta \left(z_h - \frac{\omega_h}{\omega_J} \right) \langle 0 | \delta(\omega - \bar{n} \cdot \mathcal{P}) \delta^2(\mathcal{P}_\perp - \mathbf{j}_\perp) \\ & \times \mathcal{B}_{n\perp\mu}(0) | (Jh)X \rangle \langle (Jh)X | \mathcal{B}_{n\perp}^\mu(0) | 0 \rangle, \end{aligned} \quad (2.1b)$$

where N_c is the number of the colors for quarks, and \mathbf{j}_\perp is the transverse momentum of the hadron h with respect to the standard jet axis. The large light-cone momentum components of the initial parton c , the jet, and the hadron h are given by ω , ω_J , ω_h , respectively. We choose to express the results of our calculation in terms of the following ratios of these variables

$$z = \frac{\omega_J}{\omega}, \quad z_h = \frac{\omega_h}{\omega_J}, \quad (2.2)$$

as well as ω_J which is related to the transverse momentum of the reconstructed jet. In Eq. (2.1), we have $n^\mu = (1, \hat{n})$ and $\bar{n}^\mu = (1, -\hat{n})$ where the spatial component \hat{n} is chosen along the standard jet axis. In addition, we have $n^2 = \bar{n}^2 = 0$ and $n \cdot \bar{n} = 2$. The gauge invariant collinear quark and gluon fields within Soft Collinear Effective Theory (SCET) [17–21] are denoted by χ_n and $\mathcal{B}_{n\perp}^\mu$ as usual, and \mathcal{P} is the label momentum operator. The sum over states $|X\rangle$ runs over all final state particles except for the observed jet J with the identified hadron h inside.

In [16, 22], it was found that the characteristic momentum scale for the jet dynamics with a jet radius R is given by

$$\mu_J \sim \omega_J \tan(R/2). \quad (2.3)$$

We would like to point out that for the standard jet algorithms in pp collisions, one can simply make the replacement $\omega_J \tan(R/2) \rightarrow p_T R$, where the jet size R is defined in the (η, ϕ) plane, see e.g. Ref. [23, 24]. Depending on the relative scaling of j_\perp , μ_J and Λ_{QCD} one finds different factorization theorems for the hadron-in-jet cross section.

First, we consider the case when j_\perp is of the same order as the characteristic jet scale μ_J , i.e., $\Lambda_{\text{QCD}} \ll j_\perp \sim p_T R$. In this case, the siTMDFJF \mathcal{G}_c^h as defined in Eq. (2.1) can be factorized into standard collinear fragmentation functions $D_{h/i}(z_h, \mu)$ convolved with Wilson coefficients in z_h [9, 25]. The Wilson coefficients are functions of z , ω_J and j_\perp , and can be calculated perturbatively.

Second, in the region where j_\perp is much smaller than the characteristic jet scale μ_J , i.e., $\Lambda_{\text{QCD}} \lesssim j_\perp \ll p_T R$, the perturbative expansion is plagued with large logarithmic corrections of the form $\ln(p_T R/j_\perp)$, and the standard collinear factorization breaks down. Therefore, in the small j_\perp regime, a new factorization formalism – TMD factorization [26], is required to recover reliable predictions within QCD perturbation theory. This is the kinematic region that we address in this work.

2.2 Factorization theorem

We focus on the kinematic region with the relative scalings $\Lambda_{\text{QCD}} \lesssim j_\perp \ll p_T R$, referred to as a TMD region. In this region, since the transverse momentum j_\perp inside the jet is

parametrically small, only collinear radiation within the jet with the momentum scaling $p_c = (p_c^-, p_c^+, p_{c\perp}) \sim p_T(1, \lambda^2, \lambda)$ where $\lambda \sim j_\perp/p_T$, and the soft radiation of order j_\perp are relevant to leading power of the cross section.¹ Harder emissions are only allowed outside the jet and, therefore, do not affect the hadron transverse momentum j_\perp . Since j_\perp is defined with respect to the jet axis, any radiation outside the jet will only influence the determination of the jet axis but have no impact on the j_\perp spectrum. Therefore, we have the following factorized form for \mathcal{G}_c^h derived within SCET

$$\begin{aligned} \mathcal{G}_c^h(z, z_h, \omega_J R, \mathbf{j}_\perp, \mu) = & \mathcal{H}_{c \rightarrow i}(z, \omega_J R, \mu) \int d^2 \mathbf{k}_\perp d^2 \boldsymbol{\lambda}_\perp \delta^2(z_h \boldsymbol{\lambda}_\perp + \mathbf{k}_\perp - \mathbf{j}_\perp) \\ & \times D_{h/i}(z_h, \mathbf{k}_\perp, \mu, \nu) S_i(\boldsymbol{\lambda}_\perp, \mu, \nu R), \end{aligned} \quad (2.4)$$

where besides the usual renormalization scale μ , the scale ν arises due to the so-called rapidity divergences in the relevant functions to be discussed in detail below. Here, $\mathcal{H}_{c \rightarrow i}(z, \omega_J R, \mu)$ are hard matching functions related to out-of-jet radiation. The soft functions $S_i(\boldsymbol{\lambda}_\perp, \mu, \nu R)$ take into account soft radiation inside the jet and $D_{h/i}(z_h, \mathbf{k}_\perp, \mu, \nu)$ are the usual TMDFFs, which characterize the collinear degrees of freedom inside the jet.

The delta function relates the observed transverse momentum of the hadron \mathbf{j}_\perp to be the total transverse momentum of soft and collinear radiations. Note that $\boldsymbol{\lambda}_\perp$ is multiplied by z_h inside the delta function to account for the difference between the fragmenting parton and the observed hadron with respect to the jet axis. All the ingredients in the factorization formula will be calculated up to NLO, which determines their RG evolutions. All large logarithms of the form $\ln R$ and $\ln(p_T R/j_\perp)$ are resummed by solving the obtained RG equations and by running each component from their natural scales to the hard scale $\mu \sim p_T$ at which the cross section is evaluated.

2.3 Hard functions

The hard matching functions $\mathcal{H}_{c \rightarrow i}(z, \omega_J R, \mu)$ encode radiation with a virtuality of order $\mathcal{O}(p_T R)$ outside of the jet. They describe how an energetic parton c from the hard-scattering event produces a jet initiated by parton i with energy ω_J and radius R , and can be computed through the matching relation in Eq. (2.4). Up to NLO, they are obtained by the out-of-jet radiation diagrams for inclusive jet (substructure) observables [16]. The same hard matching functions were found in the context of central subjects measured on an inclusive jet sample in [24]. For anti- k_T jets, the renormalized expressions are given by

$$\begin{aligned} \mathcal{H}_{q \rightarrow q'}(z, \omega_J R, \mu) = & \delta_{qq'} \delta(1-z) + \delta_{qq'} \frac{\alpha_s}{2\pi} \left[C_F \delta(1-z) \left(-\frac{L^2}{2} - \frac{3}{2}L + \frac{\pi^2}{12} \right) \right. \\ & \left. + P_{qq}(z)L - 2C_F(1+z^2) \left(\frac{\ln(1-z)}{1-z} \right)_+ - C_F(1-z) \right], \end{aligned} \quad (2.5a)$$

$$\mathcal{H}_{q \rightarrow g}(z, \omega_J R, \mu) = \frac{\alpha_s}{2\pi} \left[\left(L - 2\ln(1-z) \right) P_{gq}(z) - C_F z \right], \quad (2.5b)$$

¹We note that the soft degrees of freedom considered here are the same as the coft or c-soft modes introduced in [27] and [28], respectively.

$$\begin{aligned} \mathcal{H}_{g \rightarrow g}(z, \omega_J R, \mu) &= \delta(1-z) + \frac{\alpha_s}{2\pi} \left[\delta(1-z) \left(-C_A \frac{L^2}{2} - \frac{\beta_0}{2} L + \frac{\pi^2}{12} \right) \right. \\ &\quad \left. + P_{gg}(z) L - \frac{4C_A(1-z+z^2)^2}{z} \left(\frac{\ln(1-z)}{1-z} \right)_+ \right], \end{aligned} \quad (2.5c)$$

$$\mathcal{H}_{g \rightarrow q}(z, \omega_J R, \mu) = \frac{\alpha_s}{2\pi} \left[\left(L - 2 \ln(1-z) \right) P_{qg}(z) - T_F 2z(1-z) \right], \quad (2.5d)$$

where the logarithm L is defined as

$$L = \ln \left(\frac{\mu^2}{\omega_J^2 \tan^2(R/2)} \right), \quad (2.6)$$

and the standard splitting functions are also provided here for reference

$$P_{qq}(z) = C_F \left[\frac{1+z^2}{(1-z)_+} + \frac{3}{2} \delta(1-z) \right], \quad (2.7)$$

$$P_{gq}(z) = C_F \frac{1+(1-z)^2}{z}, \quad (2.8)$$

$$P_{gg}(z) = 2C_A \left[\frac{z}{(1-z)_+} + \frac{1-z}{z} + z(1-z) \right] + \frac{\beta_0}{2} \delta(1-z), \quad (2.9)$$

$$P_{qg}(z) = T_F [z^2 + (1-z)^2]. \quad (2.10)$$

The analogous hard matching coefficients for cone jets can be found in [24]. The RG equations of the functions $\mathcal{H}_{i \rightarrow j}$ take the following form

$$\mu \frac{d}{d\mu} \mathcal{H}_{i \rightarrow j}(z, \omega_J R, \mu) = \sum_k \int_z^1 \frac{dz'}{z'} \gamma_{ik} \left(\frac{z}{z'}, \omega_J R, \mu \right) \mathcal{H}_{k \rightarrow j}(z', \omega_J R, \mu). \quad (2.11)$$

Note that this is a set of four coupled equations with a DGLAP type structure. The anomalous dimensions $\gamma_{ij}(z, \omega_J R, \mu)$ are given by

$$\gamma_{ij}(z, \omega_J R, \mu) = \delta_{ij} \delta(1-z) \Gamma_i(\omega_J R, \mu) + \frac{\alpha_s}{\pi} P_{ji}(z). \quad (2.12)$$

The second terms of the $\gamma_{ij}(z, \omega_J R, \mu)$ are the standard DGLAP evolution kernels. Instead, the first term contains a logarithm L and the functions $\Gamma_i(\omega_J R, \mu)$ are given at this order by

$$\Gamma_q(\omega_J R, \mu) = \frac{\alpha_s}{\pi} C_F \left(-L - \frac{3}{2} \right), \quad (2.13a)$$

$$\Gamma_g(\omega_J R, \mu) = \frac{\alpha_s}{\pi} C_A \left(-L - \frac{\beta_0}{2C_A} \right). \quad (2.13b)$$

To summarize, the RG equations encountered here resum double logarithms whereas the DGLAP equations are always associated with the resummation of single logarithms. Evidently, the natural scale for the hard matching coefficients $\mathcal{H}_{i \rightarrow j}(z, \omega_J R, \mu)$ is the same as the jet scale μ_J as defined in Eq. (2.3), i.e.,

$$\mu_J \sim \omega_J \tan(R/2) \rightarrow p_T R. \quad (2.14)$$

Thus, by solving the above RG equations and by evolving the hard matching functions from the scale $\mu_J \sim p_T R$ to the hard-scattering scale $\mu \sim p_T$ where the cross section is evaluated, we are resumming large logarithms of jet radius $\ln R$.

2.4 TMD fragmentation functions

Now we focus on the TMDFFs $D_{h/i}(z_h, \mathbf{k}_\perp, \mu, \nu)$, which are defined as

$$D_{h/q}(z_h, \mathbf{k}_\perp, \mu, \nu) = \frac{z_h}{2N_c} \text{Tr} \left[\frac{\not{n}}{2} \langle 0 | \delta(\omega - \bar{n} \cdot \mathcal{P}) \delta^2(\mathcal{P}_\perp - \mathbf{k}_\perp) \chi_n(0) | (Jh)X \rangle \right. \\ \left. \times \langle (Jh)X | \bar{\chi}_n(0) | 0 \rangle \right], \quad (2.15a)$$

$$D_{h/g}(z_h, \mathbf{k}_\perp, \mu, \nu) = - \frac{z_h \omega}{(d-2)(N_c^2 - 1)} \langle 0 | \delta(\omega - \bar{n} \cdot \mathcal{P}) \delta^2(\mathcal{P}_\perp - \mathbf{k}_\perp) \mathcal{B}_{n\perp\mu}(0) \rangle \\ \times | (Jh)X \rangle \langle (Jh)X | \mathcal{B}_{n\perp}^\mu(0) | 0 \rangle, \quad (2.15b)$$

where ω is the light-cone energy of the initiating quark or gluon. The TMDFFs contain rapidity divergences. We choose to employ the analytic rapidity regulator of [29] which introduces a dependence on the associated rapidity scale ν . Traditionally, TMDs are studied conveniently in Fourier transform space or b -space. Following the standard convention of Ref. [26, 30], we define the TMDFFs in b -space as

$$D_{h/i}(z_h, \mathbf{b}, \mu, \nu) = \frac{1}{z_h^2} \int d^2 \mathbf{k}_\perp e^{-i \mathbf{k}_\perp \cdot \mathbf{b} / z_h} D_{h/i}(z_h, \mathbf{k}_\perp, \mu, \nu). \quad (2.16)$$

At the same time, through the inverse Fourier transform, we obtain the TMDFFs in momentum space as

$$D_{h/i}(z_h, \mathbf{k}_\perp, \mu, \nu) = \int \frac{d^2 \mathbf{b}}{(2\pi)^2} e^{i \mathbf{k}_\perp \cdot \mathbf{b} / z_h} D_{h/i}(z_h, \mathbf{b}, \mu, \nu). \quad (2.17)$$

2.4.1 Perturbative results

In perturbation theory, the bare TMDFFs suffer from infrared (IR), ultra-violet (UV), and rapidity divergences. To understand the features of these divergences, it is instructive to study the perturbative results for the TMDFFs in the region where $k_\perp \gg \Lambda_{\text{QCD}}$. In the following, we consider perturbative splittings $i \rightarrow jk$ at the parton level, where j refers to the identified parton whose transverse momentum \mathbf{k}_\perp is measured. We denote the corresponding TMDFFs at the parton level by $D_{j/i}(z_h, \mathbf{k}_\perp, \mu, \nu)$. Up to NLO, we find the following results

$$D_{q/q}(z_h, \mathbf{k}_\perp, \mu, \nu) = \delta(1 - z_h) \delta^2(\mathbf{k}_\perp) + \frac{\alpha_s}{2\pi^2} C_F \Gamma(1 + \epsilon) e^{\epsilon \gamma_E} \frac{1}{\mu^2} \left(\frac{\mu^2}{k_\perp^2} \right)^{1+\epsilon} \\ \times \left[\frac{2z_h}{(1 - z_h)^{1+\eta}} \left(\frac{\nu}{\omega_J} \right)^\eta + (1 - \epsilon)(1 - z_h) \right], \quad (2.18a)$$

$$D_{g/q}(z_h, \mathbf{k}_\perp, \mu, \nu) = \frac{\alpha_s}{2\pi^2} C_F \Gamma(1 + \epsilon) e^{\epsilon \gamma_E} \frac{1}{\mu^2} \left(\frac{\mu^2}{k_\perp^2} \right)^{1+\epsilon} \left[\frac{1 + (1 - z_h)^2}{z_h} - \epsilon z_h \right], \quad (2.18b)$$

$$D_{g/g}(z_h, \mathbf{k}_\perp, \mu, \nu) = \delta(1 - z_h) \delta^2(\mathbf{k}_\perp) + \frac{\alpha_s}{2\pi^2} C_A \Gamma(1 + \epsilon) e^{\epsilon\gamma_E} \frac{1}{\mu^2} \left(\frac{\mu^2}{k_\perp^2} \right)^{1+\epsilon} \\ \times z_h \left[\frac{1 + z_h}{(1 - z_h)^{1+\eta}} \left(\frac{\nu}{\omega_J} \right)^\eta + (3 - 2z_h) + 2(1 - \epsilon^2) \frac{1 - z_h}{z_h^2} \right], \quad (2.18c)$$

$$D_{q/g}(z_h, \mathbf{k}_\perp, \mu, \nu) = \frac{\alpha_s}{2\pi^2} T_F \Gamma(1 + \epsilon) e^{\epsilon\gamma_E} \frac{1}{\mu^2} \left(\frac{\mu^2}{k_\perp^2} \right)^{1+\epsilon} \left[1 - \frac{2z_h(1 - z_h)}{1 - \epsilon} \right]. \quad (2.18d)$$

Note that the results for the TMDFFs here are independent of the jet radius parameter R . The allowed collinear radiation inside the jet is so collimated along the jet axis in the kinematical limit that we are considering, $j_\perp/p_T \ll R$, such that it is insensitive to the jet boundary. We now calculate the Fourier transform of these results according to Eq. (2.16). After expanding around $\eta \rightarrow 0$ and then $\epsilon \rightarrow 0$, we obtain the following results in b -space

$$D_{q/q}(z_h, \mathbf{b}, \mu, \nu) = \frac{1}{z_h^2} \left\{ \delta(1 - z_h) \right. \\ \left. + \frac{\alpha_s}{2\pi} C_F \left[\frac{2}{\eta} \left(\frac{1}{\epsilon} + \ln \left(\frac{\mu^2}{\mu_b^2} \right) \right) + \frac{1}{\epsilon} \left(2 \ln \left(\frac{\nu}{\omega_J} \right) + \frac{3}{2} \right) \right] \delta(1 - z_h) \right. \\ \left. + \frac{\alpha_s}{2\pi} \left[-\frac{1}{\epsilon} - \ln \left(\frac{\mu^2}{z_h^2 \mu_b^2} \right) \right] P_{qq}(z_h) \right. \\ \left. + \frac{\alpha_s}{2\pi} C_F \left[\ln \left(\frac{\mu^2}{\mu_b^2} \right) \left(2 \ln \left(\frac{\nu}{\omega_J} \right) + \frac{3}{2} \right) \delta(1 - z_h) + (1 - z_h) \right] \right\}, \quad (2.19a)$$

$$D_{g/q}(z_h, \mathbf{b}, \mu, \nu) = \frac{1}{z_h^2} \left\{ \frac{\alpha_s}{2\pi} \left[-\frac{1}{\epsilon} - \ln \left(\frac{\mu^2}{z_h^2 \mu_b^2} \right) \right] P_{gq}(z_h) + \frac{\alpha_s}{2\pi} C_F z_h \right\}, \quad (2.19b)$$

$$D_{g/g}(z_h, \mathbf{b}, \mu, \nu) = \frac{1}{z_h^2} \left\{ \delta(1 - z_h) \right. \\ \left. + \frac{\alpha_s}{2\pi} C_A \left[\frac{2}{\eta} \left(\frac{1}{\epsilon} + \ln \left(\frac{\mu^2}{\mu_b^2} \right) \right) + \frac{1}{\epsilon} \left(2 \ln \left(\frac{\nu}{\omega_J} \right) + \frac{\beta_0}{2C_A} \right) \right] \delta(1 - z_h) \right. \\ \left. + \frac{\alpha_s}{2\pi} \left[-\frac{1}{\epsilon} - \ln \left(\frac{\mu^2}{z_h^2 \mu_b^2} \right) \right] P_{gg}(z_h) \right. \\ \left. + \frac{\alpha_s}{2\pi} C_A \left[\ln \left(\frac{\mu^2}{\mu_b^2} \right) \left(2 \ln \left(\frac{\nu}{\omega_J} \right) + \frac{\beta_0}{2C_A} \right) \delta(1 - z_h) \right] \right\}, \quad (2.19c)$$

$$D_{q/g}(z_h, \mathbf{b}, \mu, \nu) = \frac{1}{z_h^2} \left\{ \frac{\alpha_s}{2\pi} \left[-\frac{1}{\epsilon} - \ln \left(\frac{\mu^2}{z_h^2 \mu_b^2} \right) \right] P_{qg}(z_h) + \frac{\alpha_s}{2\pi} T_F 2z_h(1 - z_h) \right\}. \quad (2.19d)$$

Here we introduced the scale μ_b which is defined as $\mu_b = 2e^{-\gamma_E}/b$ [31].

2.4.2 Renormalization

In this section we perform the renormalization of the TMDFFs and derive the resulting RG equations. We observe that the poles of $D_{q/q}$ and $D_{g/g}$ in the second lines of Eqs. (2.19a)

and (2.19c) are UV poles. Therefore, they are subtracted via the usual renormalization procedure. The bare and renormalized TMDFFs are related as

$$D_{h/i}(z_h, \mathbf{b}, \mu, \nu) = Z_i^D(\mathbf{b}, \mu, \nu) D_{h/i}^{\text{bare}}(z_h, \mathbf{b}, \mu, \nu). \quad (2.20)$$

For the relevant renormalization constants, we find

$$Z_q^D(\mathbf{b}, \mu, \nu) = 1 + \frac{\alpha_s}{2\pi} C_F \left[\frac{2}{\eta} \left(\frac{1}{\epsilon} + \ln \left(\frac{\mu^2}{\mu_b^2} \right) \right) + \frac{1}{\epsilon} \left(2 \ln \left(\frac{\nu}{\omega_J} \right) + \frac{3}{2} \right) \right], \quad (2.21a)$$

$$Z_g^D(\mathbf{b}, \mu, \nu) = 1 + \frac{\alpha_s}{2\pi} C_A \left[\frac{2}{\eta} \left(\frac{1}{\epsilon} + \ln \left(\frac{\mu^2}{\mu_b^2} \right) \right) + \frac{1}{\epsilon} \left(2 \ln \left(\frac{\nu}{\omega_J} \right) + \frac{\beta_0}{2C_A} \right) \right]. \quad (2.21b)$$

We thus obtain the associated RG equation and the rapidity renormalization group (RRG) equation

$$\mu \frac{d}{d\mu} \ln D_{h/i}(z_h, \mathbf{b}, \mu, \nu) = \gamma_{\mu,i}^D(\omega_J, \mu, \nu), \quad (2.22)$$

$$\nu \frac{d}{d\nu} \ln D_{h/i}(z_h, \mathbf{b}, \mu, \nu) = \gamma_{\nu,i}^D(b, \mu), \quad (2.23)$$

where the μ - and ν -anomalous dimensions are given by

$$\gamma_{\mu,q}^D(\omega_J, \mu, \nu) = \frac{\alpha_s}{\pi} C_F \left(2 \ln \left(\frac{\nu}{\omega_J} \right) + \frac{3}{2} \right), \quad (2.24)$$

$$\gamma_{\mu,g}^D(\omega_J, \mu, \nu) = \frac{\alpha_s}{\pi} C_A \left(2 \ln \left(\frac{\nu}{\omega_J} \right) + \frac{\beta_0}{2C_A} \right), \quad (2.25)$$

$$\gamma_{\nu,q}^D(b, \mu) = \frac{\alpha_s}{\pi} C_F \ln \left(\frac{\mu^2}{\mu_b^2} \right), \quad (2.26)$$

$$\gamma_{\nu,g}^D(b, \mu) = \frac{\alpha_s}{\pi} C_A \ln \left(\frac{\mu^2}{\mu_b^2} \right). \quad (2.27)$$

2.4.3 Matching onto collinear FFs

After the UV poles are removed via renormalization, the TMDFFs $D_{j/i}(z_h, \mathbf{b}, \mu, \nu)$ only contain IR poles which have the expected structure $\sim -1/\epsilon P_{ji}(z_h)$. In the perturbative region $1/b \gg \Lambda_{\text{QCD}}$, the TMDFFs can be further matched onto the standard collinear FFs $D_{h/i}(z_h, \mu)$. With the help of this matching procedure, the remaining IR poles can be subtracted. The matching relation is given by

$$D_{h/i}(z_h, \mathbf{b}, \mu, \nu) = \frac{1}{z_h^2} \int_{z_h}^1 \frac{d\hat{z}_h}{\hat{z}_h} \tilde{C}_{j \leftarrow i} \left(\frac{z_h}{\hat{z}_h}, \mathbf{b}, \mu, \nu \right) D_{h/j}(\hat{z}_h, \mu) \equiv \frac{1}{z_h^2} \tilde{C}_{j \leftarrow i} \otimes D_{h/j}(z_h, \mu), \quad (2.28)$$

where the matching coefficients are denoted by $\tilde{C}_{j \leftarrow i}$. The perturbative results at the parton level for the collinear FFs $D_{j/i}(z_h, \mu)$ in the $\overline{\text{MS}}$ scheme are given by

$$D_{j/i}(z_h, \mu) = \delta_{ij} \delta(1 - z_h) + \frac{\alpha_s}{2\pi} \left(-\frac{1}{\epsilon} \right) P_{ji}(z_h). \quad (2.29)$$

Together with the expressions for the TMDFFs in Eq. (2.19), we find that the matching coefficients in b -space are given by

$$\begin{aligned} \tilde{C}_{q' \leftarrow q}(z_h, \mathbf{b}, \mu, \nu) = & \delta_{qq'} \left\{ \delta(1 - z_h) - \frac{\alpha_s}{2\pi} \ln \left(\frac{\mu^2}{z_h^2 \mu_b^2} \right) P_{qq}(z_h) \right. \\ & \left. + \frac{\alpha_s}{2\pi} C_F \left[\ln \left(\frac{\mu^2}{\mu_b^2} \right) \left(2 \ln \left(\frac{\nu}{\omega_J} \right) + \frac{3}{2} \right) \delta(1 - z_h) + (1 - z_h) \right] \right\}, \end{aligned} \quad (2.30a)$$

$$\tilde{C}_{g \leftarrow q}(z_h, \mathbf{b}, \mu, \nu) = \frac{\alpha_s}{2\pi} \left[- \ln \left(\frac{\mu^2}{z_h^2 \mu_b^2} \right) P_{gq}(z_h) + C_F z_h \right], \quad (2.30b)$$

$$\begin{aligned} \tilde{C}_{g \leftarrow g}(z_h, \mathbf{b}, \mu, \nu) = & \delta(1 - z_h) - \frac{\alpha_s}{2\pi} \ln \left(\frac{\mu^2}{z_h^2 \mu_b^2} \right) P_{gg}(z_h) \\ & + \frac{\alpha_s}{2\pi} C_A \left[\ln \left(\frac{\mu^2}{\mu_b^2} \right) \left(2 \ln \left(\frac{\nu}{\omega_J} \right) + \frac{\beta_0}{2C_A} \right) \delta(1 - z_h) \right], \end{aligned} \quad (2.30c)$$

$$\tilde{C}_{q \leftarrow g}(z_h, \mathbf{b}, \mu, \nu) = \frac{\alpha_s}{2\pi} \left[- \ln \left(\frac{\mu^2}{z_h^2 \mu_b^2} \right) P_{gq}(z_h) + \frac{1}{2} T_F z_h (1 - z_h) \right]. \quad (2.30d)$$

2.5 Soft functions

The soft function $S_i(\boldsymbol{\lambda}_\perp, \mu, \nu R)$ is defined as

$$S(\boldsymbol{\lambda}_\perp, \mu, \nu R) = \langle 0 | \bar{Y}_n \delta^2 (\mathcal{P}_\perp^{\epsilon J} - \boldsymbol{\lambda}_\perp) Y_n | X \rangle \langle X | \bar{Y}_n Y_n | 0 \rangle, \quad (2.31)$$

where $Y_{n(\bar{n})}$ denotes the soft Wilson line, and $\mathcal{P}_\perp^{\epsilon J}$ indicates the fact that only the soft radiation inside the jet contributes to the hadron transverse momentum with respect to the jet axis. The soft functions $S_i(\boldsymbol{\lambda}_\perp, \mu, \nu R)$ also contain rapidity divergences and, thus, the rapidity scale ν arises. The calculation of the soft functions in the perturbative region $\lambda_\perp \gg \Lambda_{\text{QCD}}$ is very similar to the standard global soft function that arises in the processes SIDIS, Drell-Yan, and electron-positron annihilation, except that now we restrict the soft radiation to be inside the jet. The final result up to NLO in momentum space is given by

$$\begin{aligned} S_i(\boldsymbol{\lambda}_\perp, \mu, \nu R) = & \delta^2(\boldsymbol{\lambda}_\perp) + C_i \frac{\alpha_s}{\pi^2} e^{\gamma_E \epsilon} \frac{\Gamma(1 + \epsilon + \frac{\eta}{2})}{\Gamma(1 + \frac{\eta}{2})} \frac{1}{\mu^2} \left(\frac{\mu^2}{\lambda_\perp^2} \right)^{1 + \epsilon + \frac{\eta}{2}} \\ & \times \frac{1}{\eta} \left(\frac{\nu \tan(R/2)}{\mu} \right)^\eta \left[1 + \mathcal{O}(R^2) \right], \end{aligned} \quad (2.32)$$

where we keep the leading contribution in the limit $R \ll 1$. The color factors are given by $C_i = C_F (C_A)$ for $i = q (g)$, respectively. After taking the Fourier transform to b -space, we obtain

$$\begin{aligned} S_i(\mathbf{b}, \mu, \nu R) = & \int d^2 \boldsymbol{\lambda}_\perp e^{-i \boldsymbol{\lambda}_\perp \cdot \mathbf{b}} S_i(\boldsymbol{\lambda}_\perp, \mu, \nu R) \\ = & 1 + \frac{\alpha_s}{2\pi} C_i \left[\frac{2}{\eta} \left(-\frac{1}{\epsilon} - \ln \left(\frac{\mu^2}{\mu_b^2} \right) \right) + \frac{1}{\epsilon^2} - \frac{1}{\epsilon} \ln \left(\frac{\nu^2 \tan^2(R/2)}{\mu^2} \right) \right] \end{aligned}$$

$$-\ln\left(\frac{\mu^2}{\mu_b^2}\right)\ln\left(\frac{\nu^2\tan^2(R/2)}{\mu_b^2}\right)+\frac{1}{2}\ln^2\left(\frac{\mu^2}{\mu_b^2}\right)-\frac{\pi^2}{12}]. \quad (2.33)$$

Note that the same result was obtained in [24] in the context of central subsets. Similar to the renormalization of the TMDFs discussed above, we subtract the UV poles of the soft functions. The renormalized and bare soft functions $S_i(\mathbf{b}, \mu, \nu R)$ are related by

$$S_i(\mathbf{b}, \mu, \nu R) = Z_i^S(\mathbf{b}, \mu, \nu) S_i^{\text{bare}}(\mathbf{b}, \mu, \nu R), \quad (2.34)$$

where the multiplicative renormalization constants Z_i^S are given by

$$Z_i^S(\mathbf{b}, \mu, \nu) = 1 + \frac{\alpha_s}{2\pi} C_i \left[\frac{2}{\eta} \left(-\frac{1}{\epsilon} - \ln\left(\frac{\mu^2}{\mu_b^2}\right) \right) + \frac{1}{\epsilon^2} - \frac{1}{\epsilon} \ln\left(\frac{\nu^2\tan^2(R/2)}{\mu^2}\right) \right]. \quad (2.35)$$

The associated RG and RRG equations are given by

$$\mu \frac{d}{d\mu} \ln S_i(\mathbf{b}, \mu, \nu R) = \gamma_{\mu,i}^S(b, \mu, \nu R), \quad (2.36)$$

$$\nu \frac{d}{d\nu} \ln S_i(\mathbf{b}, \mu, \nu R) = \gamma_{\nu,i}^S(b, \mu), \quad (2.37)$$

with the μ - and ν -anomalous dimensions

$$\gamma_{\mu,i}^S(b, \mu, \nu R) = -\frac{\alpha_s}{\pi} C_i \ln\left(\frac{\nu^2\tan^2(R/2)}{\mu_b^2}\right), \quad (2.38)$$

$$\gamma_{\nu,i}^S(b, \mu) = -\frac{\alpha_s}{\pi} C_i \ln\left(\frac{\mu^2}{\mu_b^2}\right). \quad (2.39)$$

2.6 Solution of the evolution equations and resummation

In this section, we provide the details about how to solve the RG and RRG equations derived above for three functions of the siTMDFJFs, i.e. the hard matching functions, the TMDFs and the soft functions. The resummation of all large logarithms is obtained by the following two step process. First, we evaluate all fixed order results at their natural scales which eliminates all large logarithms. Second, we evolve all three functions from their natural scales to a common scale $\mu \sim p_T$. Effectively, this procedure resums all large logarithms in the fixed-order results derived above. We are going to find that it is numerically more convenient to evolve the TMDFs and the soft functions to the jet scale $\mu \sim p_T R$ and to combine the result at this scale with the hard matching functions to obtain the siTMDFJFs. Then, we evolve the thus obtained siTMDFJFs from $p_T R \rightarrow p_T$ using the RG equations for the combined siTMDFJFs rather than using the RG equations for the three separate functions. We are going to find that the siTMDFJFs satisfy the timelike DGLAP evolution equations like their collinear analogous, the semi-inclusive fragmenting jet functions (siFJFs) as studied in [16]. We show that both approaches for solving the RG equations are equivalent. Besides numerical simplifications, using a combined evolution for the siTMDFJFs also makes the relation to traditional TMDFs more clear. Before discussing the details of the resummation, we start by introducing the traditional definition of ‘‘proper’’ TMDs that allow for a parton model interpretation of TMD sensitive observables.

2.6.1 Proper TMD definitions

A crucial feature of the results for the TMDFFs $D_{h/i}$ and the soft functions S_i is that both have rapidity divergences, but their product $D_{h/i}S_i$ is free of rapidity divergences as they exactly cancel. This can be seen clearly from the NLO expressions for $D_{h/i}$ in Eq. (2.19) and S_i in Eq. (2.33). The same $1/\eta$ poles appear in both expressions but with opposite signs. Following the usual TMD phenomenology [26, 31, 32], we thus define the “proper” in-jet TMDFFs $\mathcal{D}_{h/i}^R$ as the product

$$\mathcal{D}_{h/i}^R(z_h, \mathbf{b}; \mu) \equiv D_{h/i}(z_h, \mathbf{b}, \mu, \nu) S_i(\mathbf{b}, \mu, \nu R), \quad (2.40)$$

where the superscript R reminds us that it represents the hadron distribution within a jet of the radius R . The cancelation of rapidity divergences for $\mathcal{D}_{h/i}^R$ can be traced back to the fact that the soft radiation is restricted to be only inside the jet. Note that the TMDFFs $D_{h/i}$ for the in-jet calculation turned out to be the same as for other TMD sensitive observables [26, 31, 32] and they do not depend on R , as discussed above. However, the soft functions are different in the sense that the soft radiation is restricted to be only inside the jet. Instead, for the “global” soft functions that are relevant for SIDIS and electron-positron annihilation [33–35], there is no such phase space constraint. The additional phase space restriction encountered here cuts off half of the rapidity divergences compared to the global soft functions. This leads to the cancelation of the rapidity divergences in Eq. (2.40) for the product $\mathcal{D}_{h/i}^R = D_{h/i}S_i$.

To be more specific, we present results for the global soft functions as well. We use $\hat{S}_i(\mathbf{b}, \mu, \nu)$ to denote the global soft function in Fourier transform space. Without any phase space constraints on the soft radiation, we obtain the following expression for the global soft function in momentum space [29, 36]

$$\begin{aligned} \hat{S}_i(\boldsymbol{\lambda}_\perp, \mu, \nu) &= \delta^2(\boldsymbol{\lambda}_\perp) + C_i \frac{\alpha_s}{\pi^2} e^{\gamma_E \epsilon} \frac{\Gamma(1 + \epsilon + \frac{\eta}{2})}{\Gamma(1 + \frac{\eta}{2})} \frac{1}{\mu^2} \left(\frac{\mu^2}{\lambda_\perp^2} \right)^{1 + \epsilon + \frac{\eta}{2}} \\ &\times \left(\frac{\nu}{\mu} \right)^\eta \frac{2^{-\eta} \Gamma(\frac{1-\eta}{2}) \Gamma(\frac{\eta}{2})}{\sqrt{\pi}}. \end{aligned} \quad (2.41)$$

After taking the Fourier transform to b -space as in Eq. (2.33) and expanding around $\eta, \epsilon \rightarrow 0$, we find

$$\begin{aligned} \hat{S}_i(\mathbf{b}, \mu, \nu) &= 1 + \frac{\alpha_s}{2\pi} C_i \left[\frac{4}{\eta} \left(-\frac{1}{\epsilon} - \ln \left(\frac{\mu^2}{\mu_b^2} \right) \right) + \frac{2}{\epsilon^2} - \frac{2}{\epsilon} \ln \left(\frac{\nu^2}{\mu^2} \right) \right. \\ &\quad \left. - 2 \ln \left(\frac{\mu^2}{\mu_b^2} \right) \ln \left(\frac{\nu^2}{\mu_b^2} \right) + \ln^2 \left(\frac{\mu^2}{\mu_b^2} \right) - \frac{\pi^2}{6} \right]. \end{aligned} \quad (2.42)$$

Comparing this result with the $S_i(\mathbf{b}, \mu, \nu R)$ in Eq. (2.33), we find that the $\mathcal{O}(\alpha_s)$ terms differ by an overall factor of 2 and $\nu \leftrightarrow \nu \tan(R/2)$. The “proper” standard TMDFFs $\hat{\mathcal{D}}_{h/i}$ as they appear in SIDIS and electron-positron annihilation are then defined as

$$\hat{\mathcal{D}}_{h/i}(z_h, \mathbf{b}; \mu) \equiv D_{h/i}(z_h, \mathbf{b}, \mu, \nu) \sqrt{\hat{S}_i(\mathbf{b}, \mu, \nu)}. \quad (2.43)$$

This product is also free of rapidity divergences allowing for a parton model type interpretation of TMD sensitive observables [26, 31, 32]. It is important to work out the exact relation between the in-jet TMDFFs $\mathcal{D}_{h/i}^R$ considered in this work and the standard TMDFFs $\hat{\mathcal{D}}_{h/i}$. We will discuss this relation in more detail after deriving the solution of the RG and RRG equations in the next section.

2.6.2 Hard matching functions

We start with the RG equations for the hard matching functions $\mathcal{H}_{i \rightarrow j}$, see Eq. (2.11). Note that the anomalous dimensions $\gamma_{ij}(z, \omega_J R, \mu)$ in Eq. (2.12) contain a purely diagonal piece $\delta_{ij} \delta(1-z) \Gamma_i(\omega_J R, \mu)$ and the Altarelli-Parisi splitting functions $P_{ji}(z)$ similar to the timelike DGLAP. We are going to separate these two parts of the anomalous dimensions and the associated evolution. The purely diagonal or non-DGLAP pieces of $\gamma_{ij}(z, \omega_J R, \mu)$ are going to cancel with the respective terms of the anomalous dimensions of the TMDFFs and the soft functions yielding a standard DGLAP evolution equation for the siTMDFFs. To that extend, we start by writing the functions $\mathcal{H}_{i \rightarrow j}$ as

$$\mathcal{H}_{i \rightarrow j}(z, \omega_J R, \mu) = \mathcal{E}_i(\omega_J R, \mu) \mathcal{C}_{i \rightarrow j}(z, \omega_J R, \mu), \quad (2.44)$$

where the $\mathcal{C}_{i \rightarrow j}(z, \omega_J R, \mu)$ satisfy evolution equations where the anomalous dimensions are given only by the Altarelli-Parisi splitting functions

$$\mu \frac{d}{d\mu} \mathcal{C}_{i \rightarrow j}(z, \omega_J R, \mu) = \frac{\alpha_s}{2\pi} \sum_k \int_z^1 \frac{dz'}{z'} P_{ki} \left(\frac{z}{z'} \right) \mathcal{C}_{k \rightarrow j}(z', \omega_J R, \mu). \quad (2.45)$$

Note that these evolution equations are similar to DGLAP equations but here we still have four coupled equations. Only the combined siTMDFFs are going to satisfy the standard timelike DGLAP evolution equations, see Eq. (2.71) below.

The functions $\mathcal{E}_i(\omega_J R, \mu)$ satisfy multiplicative RG equations

$$\mu \frac{d}{d\mu} \ln \mathcal{E}_i(\omega_J R, \mu) = \Gamma_i(\omega_J R, \mu), \quad (2.46)$$

where the $\Gamma_i(\omega_J R, \mu)$ are given in Eq. (2.13). The solution for the multiplicative RG equations can be written as

$$\mathcal{E}_i(\omega_J R, \mu) = \mathcal{E}_i(\omega_J R, \mu_J) \exp \left(\int_{\mu_J}^{\mu} \frac{d\mu'}{\mu'} \Gamma_i(\omega_J R, \mu') \right). \quad (2.47)$$

The fixed-order results for $\mathcal{E}_i(\omega_J R, \mu)$ can be obtained from Eq. (2.5) and are given by

$$\mathcal{E}_q(\omega_J R, \mu) = 1 + \frac{\alpha_s}{2\pi} C_F \left(-\frac{L^2}{2} - \frac{3}{2} L \right), \quad (2.48a)$$

$$\mathcal{E}_g(\omega_J R, \mu) = 1 + \frac{\alpha_s}{2\pi} \left(-C_A \frac{L^2}{2} - \frac{\beta_0}{2} L \right). \quad (2.48b)$$

By choosing $\mu_J = p_T R$, we obtain $\mathcal{E}_i(\omega_J R, \mu_J) = 1$ as the initial condition for the evolution in Eq. (2.46). Using this result in Eq. (2.44) above, we can write the hard matching functions as

$$\mathcal{H}_{i \rightarrow j}(z, \omega_J R, \mu) = \exp \left(\int_{\mu_J}^{\mu} \frac{d\mu'}{\mu'} \Gamma_i(\omega_J R, \mu') \right) \mathcal{C}_{i \rightarrow j}(z, \omega_J R, \mu). \quad (2.49)$$

The functions $\mathcal{C}_{i \rightarrow j}(z, \omega_J R, \mu)$ still need to be evolved from $\mu \sim \mu_J = p_T R$ to $\mu \sim p_T$ using the evolution equations in Eq. (2.45) above. Their fixed order expressions are given by

$$\begin{aligned} \mathcal{C}_{q \rightarrow q'}(z, \omega_J R, \mu) = & \delta_{qq'} \delta(1-z) + \delta_{qq'} \frac{\alpha_s}{2\pi} \left[C_F \delta(1-z) \frac{\pi^2}{12} + P_{qq}(z) L \right. \\ & \left. - 2C_F(1+z^2) \left(\frac{\ln(1-z)}{1-z} \right)_+ - C_F(1-z) \right], \end{aligned} \quad (2.50a)$$

$$\mathcal{C}_{q \rightarrow g}(z, \omega_J R, \mu) = \frac{\alpha_s}{2\pi} \left[\left(L - 2 \ln(1-z) \right) P_{gq}(z) - C_F z \right], \quad (2.50b)$$

$$\mathcal{C}_{g \rightarrow g}(z, \omega_J R, \mu) = \delta(1-z) + \frac{\alpha_s}{2\pi} \left[\delta(1-z) \frac{\pi^2}{12} + P_{gg}(z) L - \frac{4C_A(1-z+z^2)^2}{z} \left(\frac{\ln(1-z)}{1-z} \right)_+ \right], \quad (2.50c)$$

$$\mathcal{C}_{g \rightarrow q}(z, \omega_J R, \mu) = \frac{\alpha_s}{2\pi} \left[\left(L - 2 \ln(1-z) \right) P_{qg}(z) - T_F 2z(1-z) \right]. \quad (2.50d)$$

2.6.3 Relation between in-jet and standard TMDFFs

We are now going to derive the solution of the evolution equations for the TMDFFs and the soft functions in order to obtain the proper in-jet TMDFFs $\mathcal{D}_{h/i}^R(z_h, \mathbf{b}; \mu)$ as defined in Eq. (2.40). For comparison, we also show the results for the standard TMDFFs $\hat{\mathcal{D}}_{h/i}(z_h, \mathbf{b}; \mu)$ as in Eq. (2.43). We start by evolving $D_{h/i}(z_h, \mathbf{b}, \mu, \nu)$, $S_i(\mathbf{b}, \mu, \nu, R)$ and $\hat{S}_i(\mathbf{b}, \mu, \nu)$ using their RG and RRG equations. From the perturbative calculations above, we find that the natural scales for the TMDFFs $D_{h/i}$, and the two soft functions S_i, \hat{S}_i are given by

$$\mu_D \sim \mu_b, \quad \nu_D \sim \omega_J, \quad (2.51a)$$

$$\mu_S \sim \mu_b, \quad \nu_S \sim \frac{\mu_b}{\tan(R/2)}, \quad (2.51b)$$

$$\mu_{\hat{S}} \sim \mu_b, \quad \nu_{\hat{S}} \sim \mu_b. \quad (2.51c)$$

To be consistent with the standard Collins-Soper-Sterman (CSS) formalism [37], we evolve from the natural scales of $D_{h/i}$ and S_i, \hat{S}_i as given in Eq. (2.51), to a common scale μ and ν . In terms of the ‘‘proper’’ TMDFFs in (2.40), the initial conditions for the evolution is given by

$$\mathcal{D}_{h/i}^R(z_h, \mathbf{b}; \mu_b) \equiv D_{h/i}(z_h, \mathbf{b}, \mu_D, \nu_D) S_i(\mathbf{b}, \mu_S, \nu_S R), \quad (2.52)$$

$$\hat{\mathcal{D}}_{h/i}(z_h, \mathbf{b}; \mu_b) \equiv D_{h/i}(z_h, \mathbf{b}, \mu_D, \nu_D) \sqrt{\hat{S}_i(\mathbf{b}, \mu_{\hat{S}}, \nu_{\hat{S}})}. \quad (2.53)$$

It might be instructive to point out that the ‘‘proper’’ TMDs chosen as such are equal perturbatively when evaluated at their natural scales,

$$\mathcal{D}_{h/i}^R(z_h, \mathbf{b}; \mu_b) = \hat{\mathcal{D}}_{h/i}(z_h, \mathbf{b}; \mu_b). \quad (2.54)$$

This can be directly verified from the perturbative expressions given above. At this point, it might be instructive to point out that according to Eq. (2.51), the natural rapidity scales

for two soft functions S_i and \hat{S}_i are quite different, $\nu_S/\nu_{\hat{S}} = 1/\tan(R/2) \gg 1$ in the small jet radius limit $R \ll 1$. Since the ‘‘proper’’ TMDs do not contain rapidity divergences anymore, the ν -dependence will naturally disappear in the end when one evolves to the common rapidity scales. After solving the corresponding RG and RRG equations, we can write the final result in the following form

$$\mathcal{D}_{h/i}^R(z_h, \mathbf{b}; \mu) = \mathcal{D}_{h/i}^R(z_h, \mathbf{b}; \mu_b) \exp \left[- \int_{\mu_b}^{\mu} \frac{d\mu'}{\mu'} \left(\Gamma_{\text{cusp}}^i \ln \left(\frac{\mu_J^2}{\mu'^2} \right) + \gamma^i \right) \right], \quad (2.55)$$

$$\hat{\mathcal{D}}_{h/i}(z_h, \mathbf{b}; \mu) = \hat{\mathcal{D}}_{h/i}(z_h, \mathbf{b}; \mu_b) \exp \left[- \int_{\mu_b}^{\mu} \frac{d\mu'}{\mu'} \left(\Gamma_{\text{cusp}}^i \ln \left(\frac{\mu^2}{\mu'^2} \right) + \gamma^i \right) \right]. \quad (2.56)$$

Here the cusp anomalous dimension Γ_{cusp}^i and the non-cusp γ^i allow for a perturbative evaluation as $\Gamma_{\text{cusp}}^i = \sum_n \Gamma_{n-1}^i \left(\frac{\alpha_s}{\pi} \right)^n$ and likewise for γ^i . The first coefficients can be obtained from our calculation and are given by

$$\Gamma_0^q = C_F, \quad \gamma_0^q = -\frac{3}{2}C_F, \quad (2.57)$$

$$\Gamma_0^g = C_A, \quad \gamma_0^g = -\frac{\beta_0}{2}. \quad (2.58)$$

The higher-order expressions can be found for example in Ref. [38]. The ‘‘proper’’ in-jet TMDs $\mathcal{D}_{h/i}^R$ in Eq. (2.55) may be further expressed in terms of the ‘‘proper’’ standard TMDs $\hat{\mathcal{D}}_{h/i}$ in Eq. (2.56) as

$$\begin{aligned} \mathcal{D}_{h/i}^R(z_h, \mathbf{b}; \mu) &= \mathcal{D}_{h/i}^R(z_h, \mathbf{b}; \mu_b) \exp \left[- \int_{\mu_b}^{\mu_J} \frac{d\mu'}{\mu'} \left(\Gamma_{\text{cusp}}^i \ln \left(\frac{\mu_J^2}{\mu'^2} \right) + \gamma^i \right) \right] \\ &\quad \times \exp \left[- \int_{\mu_J}^{\mu} \frac{d\mu'}{\mu'} \left(\Gamma_{\text{cusp}}^i \ln \left(\frac{\mu_J^2}{\mu'^2} \right) + \gamma^i \right) \right] \\ &= \hat{\mathcal{D}}_{h/i}(z_h, \mathbf{b}; \mu_J) \exp \left[- \int_{\mu_J}^{\mu} \frac{d\mu'}{\mu'} \left(\Gamma_{\text{cusp}}^i \ln \left(\frac{\mu_J^2}{\mu'^2} \right) + \gamma^i \right) \right]. \end{aligned} \quad (2.59)$$

To obtain the second line we made use of Eq. (2.54). In other words, the evolved ‘‘proper’’ TMDs obtained for the hadron distribution inside jets $\mathcal{D}_{h/i}^R(z_h, \mathbf{b}; \mu)$ at scale μ is related to the standard TMDs $\hat{\mathcal{D}}_{h/i}(z_h, \mathbf{b}; \mu_J)$ evaluated at scale μ_J multiplied by an overall factor. This overall factor is given by an exponential involving an integration over μ' from scales μ_J to μ . Since scales μ_J and μ are both in the perturbative regime, $\mu_J, \mu \gg \Lambda_{\text{QCD}}$, we find that the relation between the in-jet TMDs $\mathcal{D}_{h/i}^R$ and the standard TMDs $\hat{\mathcal{D}}_{h/i}$ is purely perturbative.

2.6.4 Solution for the siTMDFJFs

We proceed by combining the above results in order to obtain the evolved siTMDFJFs $\mathcal{G}_c^h(z, z_h, \omega_J R, \mathbf{j}_\perp, \mu)$. Starting from Eq. (2.4) and by using the relation

$$\delta^2(z_h \boldsymbol{\lambda}_\perp + \mathbf{k}_\perp - \mathbf{j}_\perp) = \frac{1}{z_h^2} \int \frac{d^2 \mathbf{b}}{(2\pi)^2} \exp \left(-i \left(\boldsymbol{\lambda}_\perp + \frac{\mathbf{k}_\perp}{z_h} - \frac{\mathbf{j}_\perp}{z_h} \right) \cdot \mathbf{b} \right), \quad (2.60)$$

one finds

$$\begin{aligned}\mathcal{G}_c^h(z, z_h, \omega_J R, \mathbf{j}_\perp, \mu) &= \mathcal{H}_{c \rightarrow i}(z, \omega_J R, \mu) \int \frac{d^2 \mathbf{b}}{(2\pi)^2} e^{i \mathbf{j}_\perp \cdot \mathbf{b} / z_h} D_{h/i}(z_h, \mathbf{b}, \mu, \nu) S_i(\mathbf{b}, \mu, \nu R) \\ &= \mathcal{H}_{c \rightarrow i}(z, \omega_J R, \mu) \int \frac{d^2 \mathbf{b}}{(2\pi)^2} e^{i \mathbf{j}_\perp \cdot \mathbf{b} / z_h} \mathcal{D}_{h/i}^R(z_h, \mathbf{b}; \mu).\end{aligned}\quad (2.61)$$

Now we can plug in the result of the hard matching coefficients $\mathcal{H}_{c \rightarrow i}(z, \omega_J R, \mu)$ in Eq. (2.49) where we separated and solved the RG equations for the functions $\mathcal{E}_i(\omega_J R, \mu)$. In addition, we use the results of the evolved in-jet TMDs $\mathcal{D}_{h/i}^R(z_h, \mathbf{b}; \mu)$ in Eq. (2.59). We find that the siTMDFJFs may eventually be expressed as

$$\mathcal{G}_c^h(z, z_h, \omega_J R, \mathbf{j}_\perp, \mu) = \mathcal{C}_{c \rightarrow i}(z, \omega_J R, \mu) \int \frac{d^2 \mathbf{b}}{(2\pi)^2} e^{i \mathbf{j}_\perp \cdot \mathbf{b} / z_h} \hat{\mathcal{D}}_{h/i}(z_h, \mathbf{b}; \mu_J). \quad (2.62)$$

It is important to note that here we are able to write the result in terms of the standard TMDs $\hat{\mathcal{D}}_{h/i}$. This is possible since the evolution between the scales μ_J and μ of $\mathcal{E}_i(\omega_J R, \mu)$ cancels with the overall multiplicative factor found in Eq. (2.59) for the in-jet TMDs when written in terms of the standard TMDs. Specifically, we have

$$\exp\left(\int_{\mu_J}^{\mu} \frac{d\mu'}{\mu'} \Gamma_i(\omega_J R, \mu')\right) \exp\left[-\int_{\mu_J}^{\mu} \frac{d\mu'}{\mu'} \left(\Gamma_{\text{cusp}}^i \ln\left(\frac{\mu_J^2}{\mu'^2}\right) + \gamma^i\right)\right] = 1. \quad (2.63)$$

The result in Eq. (2.62) constitutes the most important part of our work. It explicitly demonstrates that the hadron transverse momentum distribution within jets is related to the standard TMDFFs (as measured in SIDIS and electron-positron annihilation) probed at the jet scale $\mu_J \sim p_T R$. Eventually, we can write the result as

$$\mathcal{G}_c^h(z, z_h, \omega_J R, \mathbf{j}_\perp, \mu) = \mathcal{C}_{c \rightarrow i}(z, \omega_J R, \mu) \hat{\mathcal{D}}_{h/i}(z_h, \mathbf{j}_\perp; \mu_J), \quad (2.64)$$

where we used the inverse Fourier transform as defined in Eq. (2.17) to obtain the TMDFFs in momentum space

$$\hat{\mathcal{D}}_{h/i}(z_h, \mathbf{j}_\perp; \mu_J) = \int \frac{d^2 \mathbf{b}}{(2\pi)^2} e^{i \mathbf{j}_\perp \cdot \mathbf{b} / z_h} \hat{\mathcal{D}}_{h/i}(z_h, \mathbf{b}; \mu_J). \quad (2.65)$$

2.7 Final expression for the siTMDFJFs

In the perturbative region where $1/b \gg \Lambda_{\text{QCD}}$, one can further match the TMDFFs $\hat{\mathcal{D}}_{h/i}(z_h, \mathbf{b}; \mu_b)$ onto the standard collinear FFs $D_{h/i}(z_h, \mu_b)$ as

$$\hat{\mathcal{D}}_{h/i}(z_h, \mathbf{b}; \mu_b) = \frac{1}{z_h^2} \int_{z_h}^1 \frac{d\hat{z}_h}{\hat{z}_h} C_{j \leftarrow i}\left(\frac{z_h}{\hat{z}_h}, \mu_b\right) D_{h/j}(\hat{z}_h, \mu_b). \quad (2.66)$$

Using the coefficients $\tilde{C}_{j \leftarrow i}$ given in Eq. (2.30) and the perturbative expressions for the soft functions, one obtains

$$C_{q' \leftarrow q}(z_h, \mu_b) = \delta_{qq'} \left[\delta(1 - z_h) + \frac{\alpha_s}{\pi} \left(-C_F \frac{\pi^2}{24} \delta(1 - z_h) + \frac{C_F}{2} (1 - z_h) + P_{qq}(z_h) \ln z_h \right) \right], \quad (2.67a)$$

$$C_{g\leftarrow q}(z_h, \mu_b) = \frac{\alpha_s}{\pi} \left[\frac{C_F}{2} z_h + P_{gq}(z_h) \ln z_h \right], \quad (2.67b)$$

$$C_{g\leftarrow g}(z_h, \mu_b) = \delta(1 - z_h) + \frac{\alpha_s}{\pi} \left[-C_A \frac{\pi^2}{24} \delta(1 - z_h) + P_{gg}(z_h) \ln z_h \right], \quad (2.67c)$$

$$C_{q\leftarrow g}(z_h, \mu_b) = \frac{\alpha_s}{\pi} \left[T_F z_h (1 - z_h) + P_{qg}(z_h) \ln z_h \right]. \quad (2.67d)$$

It might be instructive to point out that the above matching coefficients are computed in the standard $\overline{\text{MS}}$ scheme, which differs from the simplest minimal subtraction scheme by inserting a factor S_ϵ for each loop in the counter-terms with $S_\epsilon = (4\pi e^{-\gamma_E})^\epsilon$. However, in the so-called Collins-11 definition of TMDs, this factor was changed to $S_\epsilon^{\text{JCC}} = (4\pi)^\epsilon / \Gamma(1 - \epsilon)$ [26]. We refer to the latter scheme as $\overline{\text{MS}}^{\text{JCC}}$, in which the π^2 terms are absent in Eqs. (2.67)(a) and (c). This is compensated for by the fact that there are no π^2 -constants in the expressions for the functions $C_{i\rightarrow j}$ in Eqs. (2.50)(a) and (c) in the $\overline{\text{MS}}^{\text{JCC}}$ scheme.

So far, we have discussed the evolution of the siTMDFJFs in the perturbative region, i.e. for $1/b \gg \Lambda_{\text{QCD}}$. It is well-known that the evolution of TMDs contains a non-perturbative component in the large- b region. We treat the large- b region by adopting the usual b_* -prescription [37]. Alternative approaches can be found in [39–43]. One defines b_* as

$$b_* = \frac{b}{\sqrt{1 + b^2/b_{\text{max}}^2}}, \quad (2.68)$$

where the quantity b_{max} is introduced such that $b_* \rightarrow b$ at small $b \ll b_{\text{max}}$, whereas it approaches the limit $b \rightarrow b_{\text{max}}$ in the large b -region. Using this prescription and the matching coefficients in Eq. (2.67), we can write the evolved TMDFFs in Eq. (2.65) as

$$\hat{D}_{h/i}(z_h, \mathbf{j}_\perp; \mu_J) = \frac{1}{z_h^2} \int \frac{b db}{2\pi} J_0(j_\perp b/z) C_{j\leftarrow i} \otimes D_{h/j}(z_h, \mu_{b_*}) e^{-S_{\text{pert}}^i(b_*, \mu_J) - S_{\text{NP}}^i(b, \mu_J)}. \quad (2.69)$$

Here, $S_{\text{pert}}^i(b_*, \mu_J)$ is the perturbative Sudakov factor

$$S_{\text{pert}}^i(b_*, \mu_J) = \int_{\mu_{b_*}}^{\mu_J} \frac{d\mu'}{\mu'} \left(\Gamma_{\text{cusp}}^i \ln \left(\frac{\mu_J^2}{\mu'^2} \right) + \gamma^i \right), \quad (2.70)$$

and $S_{\text{NP}}^i(b, \mu_J)$ is the non-perturbative Sudakov factor. We will discuss them in detail in the phenomenological Sec. 3 below.

With all these relevant ingredients available, we may then compute the siTMDFJFs following Eq. (2.64). By using the evolution equations for the functions $C_{i\rightarrow j}$ in Eq. (2.45) and the expressions for siTMDFJFs in Eq. (2.64), we find that the siTMDFJFs satisfy the standard timelike DGLAP evolution equations

$$\mu \frac{d}{d\mu} \mathcal{G}_i^h(z, z_h, \omega_J R, \mathbf{j}_\perp, \mu) = \frac{\alpha_s}{2\pi} \sum_j \int_z^1 \frac{dz'}{z'} P_{ji} \left(\frac{z}{z'} \right) \mathcal{G}_j^h(z', z_h, \omega_J R, \mathbf{j}_\perp, \mu). \quad (2.71)$$

This result for the evolution equations of the siTMDFJFs was to be expected. Following our factorization expression for the differential cross section in Eq. (1.2), the product $H_{ab}^c \mathcal{G}_c^h$

should be μ -independent order by order analogously to single inclusive hadron production [44, 45]. Thus, it is natural that the \mathcal{G}_c^h follow the same DGLAP evolution equations as those for the usual collinear FFs $D_{h/c}$ [16, 22].

We would like to summarize again the following aspects of the evolution structure of the siTMDFJFs. The TMD part of the evolution between μ_b and μ_J is governed by the same TMD evolution equations that have been obtained for the standard TMDs as well. The hard matching functions $\mathcal{C}_{c \rightarrow i}$ follow RG equations where the anomalous dimensions are given by the usual Altarelli-Parisi splitting functions. The evolution of $\mathcal{C}_{c \rightarrow i}$ is carried out between the jet scale μ_J and the hard scale μ allowing for the resummation of logarithms in the jet size parameter R . The structure and resummation of single logarithms $\alpha_s^n \ln^n R$ becomes more apparent when combining both contributions to obtain the siTMDFJFs. They follow the standard DGLAP structure as it is usually associated with the resummation of single logarithms in the jet size parameter [16, 22, 46, 47]. The obtained structure for the siTMDFJFs provides a convenient method to perform the resummation of all relevant large logarithms. First, we are going to evolve the standard TMDFFs $\hat{\mathcal{D}}_{h/i}(z_h, \mathbf{j}_\perp; \mu)$ from the scale μ_b to μ_J . Second, at the jet scale μ_J the TMDFFs $\hat{\mathcal{D}}_{h/i}(z_h, \mathbf{j}_\perp; \mu_J)$ will be combined with the remaining hard matching functions $\mathcal{C}_{c \rightarrow i}(z, \omega_J R, \mu_J)$ in Eq. (2.50) to compute the siTMDFJFs $\mathcal{G}_c^h(z, z_h, \omega_J R, \mathbf{j}_\perp, \mu_J)$ as

$$\mathcal{G}_c^h(z, z_h, \omega_J R, \mathbf{j}_\perp, \mu_J) = \mathcal{C}_{c \rightarrow i}(z, \omega_J R, \mu_J) \hat{\mathcal{D}}_{h/i}(z_h, \mathbf{j}_\perp; \mu_J). \quad (2.72)$$

Then, we use the DGLAP evolution equations for the siTMDFJFs in Eq. (2.71) to evolve \mathcal{G}_c^h from the scale μ_J to μ and, thus, resum logarithms in the jet size parameter R .

3 Phenomenology for $pp \rightarrow (\text{jet}h)X$

In this section, we present numerical results for the transverse momentum distribution of hadrons inside jets for LHC kinematics. We consider an inclusive jet sample $pp \rightarrow \text{jet} + X$ where a hadron h is identified inside the reconstructed jet. Following [10, 14, 16, 22], the factorization theorem for the process $pp \rightarrow (\text{jet}h)X$ can be written as

$$\begin{aligned} \frac{d\sigma^{pp \rightarrow (\text{jet}h)X}}{dp_T d\eta dz_h d^2 \mathbf{j}_\perp} &= \sum_{a,b,c} \int_{x_a^{\min}}^1 \frac{dx_a}{x_a} f_a(x_a, \mu) \int_{x_b^{\min}}^1 \frac{dx_b}{x_b} f_b(x_b, \mu) \\ &\times \int_{z^{\min}}^1 \frac{dz}{z^2} H_{ab}^c(\hat{s}, \hat{p}_T, \hat{\eta}, \mu) \mathcal{G}_c^h(z, z_h, \omega_J R, \mathbf{j}_\perp, \mu), \end{aligned} \quad (3.1)$$

where f_a and f_b denote the parton distribution functions (PDFs) in the proton with the corresponding momentum fraction x_a and x_b , respectively. For all numerical calculations in this work, we choose the CT14 NLO set of PDFs [48]. The hard functions H_{ab}^c describe the production of an energetic parton c in the hard-scattering event. They have been calculated analytically up to NLO in [45, 49]. The variables \hat{s} , \hat{p}_T and $\hat{\eta}$ denote the partonic CM energy, and the transverse momentum and rapidity of parton c , respectively. They are related to their hadronic analogues as

$$\hat{s} = x_a x_b s, \quad \hat{p}_T = p_T / z, \quad \hat{\eta} = \eta - \ln(x_a / x_b) / 2, \quad (3.2)$$

where z is the momentum fraction transferred from parton c to the observed jet. The lower integration limits x_a^{\min} , x_b^{\min} and z^{\min} can be found for example in [14, 16]. Finally, the functions $\mathcal{G}_c^h(z_c, z_h, \omega_J R, \mathbf{j}_\perp, \mu)$ in Eq. (3.1) are the siTMDFFs as discussed in Section 2. We would like to stress that the cross section does not depend on TMDPDFs but only on the standard collinear PDFs. Unlike the TMDPDFs, collinear PDFs are very well constrained by data and have been determined in global fits in the literature. Therefore, different than for SIDIS, the hadron in-jet fragmentation considered in this work provides an opportunity to disentangle the effects of TMDPDFs and TMDFFs.

In order to perform numerical calculations, we have to parameterize the non-perturbative Sudakov factors for both quark and gluon TMDFFs. Unfortunately, the quark TMDFFs are not very well constrained so far. The main information for the extraction of quark TMDFFs are obtained from multiplicity distributions of hadrons measured in SIDIS from both the HERMES [50] and COMPASS [51] experiments. These measurements were performed at relative low momentum scales, with photon virtualities Q^2 of several GeV^2 . Thus, there are potential problems when interpreting the data in terms of the usual leading-twist TMD factorization formalism [52]. In addition, since the factorization for SIDIS involves a convolution of TMDPDFs and TMDFFs, the unambiguous extraction of both functions separately is not straightforward. Therefore, current extractions of quark TMDFFs are subject to large uncertainties. Keeping in mind the remaining large uncertainties in our calculation, we are nevertheless going to present numerical estimates for the hadron transverse momentum distribution within jets and compare to LHC measurements. We choose to use the following parametrization of the non-perturbative Sudakov factor following [53, 54]

$$S_{\text{NP}}^q(b, \mu_J) = \frac{g_2}{2} \ln\left(\frac{b}{b_*}\right) \ln\left(\frac{\mu_J}{Q_0}\right) + \frac{g_h}{z_h^2} b^2, \quad (3.3)$$

with $Q_0^2 = 2.4 \text{ GeV}^2$, $b_{\text{max}} = 1.5 \text{ GeV}^{-1}$, $g_2 = 0.84$, and $g_h = 0.042$. Other parametrizations for the non-perturbative Sudakov factor for TMDFFs have been discussed in [30, 55].

Furthermore, we note that the non-perturbative Sudakov factor for the gluon TMDFF is not constrained at all so far. For our numerical calculations, we are going to follow [56–58] and adopt a parameterization of the gluon non-perturbative Sudakov factor similar to that for quarks as

$$S_{\text{NP}}^g(b, \mu_J) = \frac{C_A}{C_F} \frac{g_2}{2} \ln\left(\frac{b}{b_*}\right) \ln\left(\frac{\mu_J}{Q_0}\right) + \frac{g_h}{z_h^2} b^2. \quad (3.4)$$

In comparison to the quark parametrization, the coefficient of the term $\sim \ln \mu_J$ is enhanced by a color factor C_A/C_F , whereas the intrinsic part $\sim g_h$ is kept unchanged.

In addition, we use the coefficients $C_{j \leftarrow i}$ in Eq. (2.67) up to the order of α_s for the TMDFFs, and keep $\Gamma_{0,1}^i$ and γ_0^i in the perturbative Sudakov factor in Eq. (2.70), which is often referred to as the next-to-leading-logarithm prime (NLL') accuracy. For both $C_{j \leftarrow i}$ in Eq. (2.67) and $\mathcal{C}_{i \rightarrow j}$ in Eq. (2.50), we use the expressions in the $\overline{\text{MS}}^{\text{JCC}}$ scheme as explained in Sec. 2.7, since the TMDFFs that we use for our numerical studies were extracted within this scheme [53, 54]. We use the DSS07 parametrization of collinear fragmentation

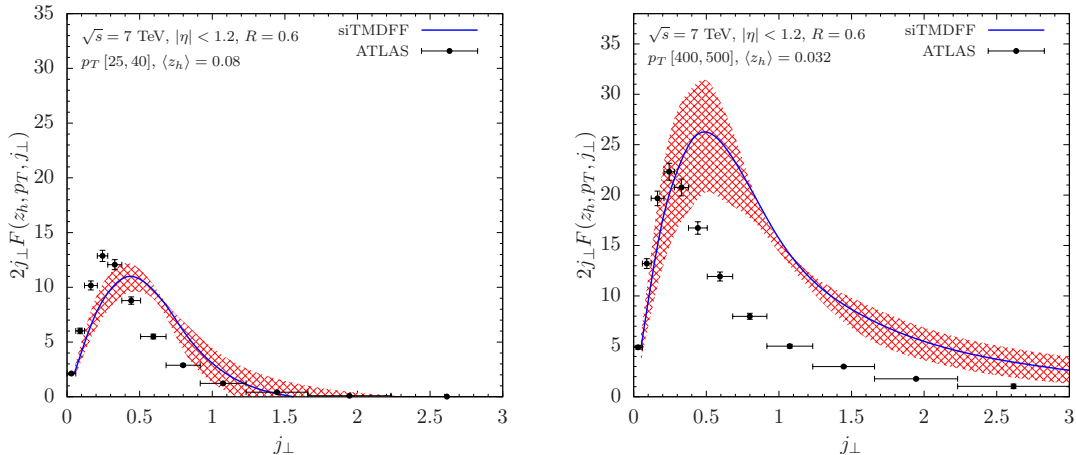


Figure 2. Hadron j_{\perp} -distributions within jets in pp collisions at $\sqrt{s} = 7$ TeV. Jets are taken into account in the rapidity interval $|\eta| < 1.2$ and they are reconstructed using the anti- k_T jet algorithm with $R = 0.6$. We choose jet transverse momentum bins $25 < p_T < 40$ GeV (left) and $400 < p_T < 500$ GeV (right). The average values $\langle z_h \rangle$ are provided by the experiment, $\langle z_h \rangle = 0.08$ (left) and 0.03 (right). The uncertainty band is calculated by varying the scales μ and μ_J independently by a factor of two around their default values $\mu = p_T$ and $\mu_J = p_T R$, and taking the envelope of these variations.

functions for light charged hadrons [59]. Together with the choices for the relevant non-perturbative inputs above for both quark and gluon TMDFFs, we are now going to present first numerical estimates for the transverse momentum distribution of hadrons inside jets and compare to the data provided by the ATLAS collaboration [3]. We choose the following jet kinematics consistent with the available data at a CM energy of $\sqrt{s} = 7$ TeV. The jets are reconstructed using the anti- k_T algorithm with jet size parameter $R = 0.6$, and the jet rapidity is integrated over $|\eta| < 1.2$. The detailed numerical implementation is very similar to the longitudinal momentum distribution of hadrons inside jets [16], using several numerical techniques developed in the literature [60–62]. The RG evolution of the various parts of the cross section is performed as outlined at the end of the last section.

In Fig. 2, we present the comparison of our numerical results and the LHC data for the hadron j_{\perp} -distribution inside jets. We make the default scale choices of $\mu = p_T$ and $\mu_J = p_T R$. We explore the scale uncertainty by varying μ and μ_J independently by a factor of two around their default values and by taking the envelope of these variations. As an example, we choose the jet transverse momentum bins $25 < p_T < 40$ GeV (left) and $400 < p_T < 500$ GeV (right). The experimental data are presented for the z_h -integrated hadron distribution, i.e. with z_h integrated from 0 to 1. This fact hinders a more direct and transparent comparison of our results with the data, since the collinear FFs are only constrained in a finite region $z_h^{\min} < z_h < 1$ with $z_h^{\min} \gtrsim 0.05$ [59, 63]. Any $z_h < z_h^{\min}$ is not constrained and can only be obtained by extrapolation. We choose the value for z_h in our calculations as the average value $\langle z_h \rangle$ that are provided in the experimental publication [3], with $\langle z_h \rangle = 0.08$ and 0.03 for $25 < p_T < 40$ GeV and $400 < p_T < 500$ GeV, respectively. With this caveat in mind, we find that our calculations based on TMDFFs

extracted in the literature at low energy scales of several GeV give a reasonable description of the experimental data. The height of the peak is roughly consistent with the data but our results have a broader j_{\perp} -distribution than the experimental data. We note that at low jet p_T our current numerical estimates agrees somewhat better with the data than in the high p_T region.

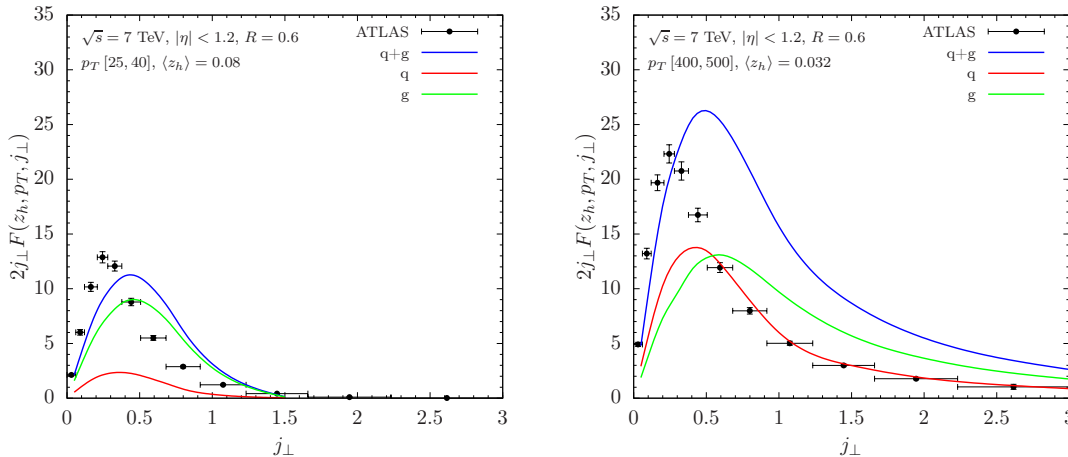


Figure 3. Breakdown of the hadron j_{\perp} -distributions inside jets (blue) into quark initiated (red) and gluon initiated (green) TMDFF channels.

In Fig. 3, we separate the hadron j_{\perp} -distribution into quark and the gluon TMDFF components. This separation is valid in the TMD region. We find that at lower jet p_T , as shown in the left panel of Fig. 3, the gluon channel dominates over the quark channel due to the overwhelmingly abundant gg initiated events in the pp collisions. The quark TMD fragmenting contribution is suppressed in this region. Therefore, the low jet p_T region provides a “golden channel” to extract the gluon TMDFF. At large jet p_T (right panel of Fig. 3), where qg initiated events start to dominate, the quark and the gluon TMDFF contributions therefore become comparable to each other. However, due to the difference in the color charges carried by quarks and gluons, the quark TMD fragmenting process peaks at smaller j_{\perp} . Away from the peak region, the quark contribution drops more dramatically and exhibits a relatively narrow spectrum compared with the gluon contribution. Therefore, the region away from the peak of the j_{\perp} -spectrum will generally be more sensitive to the gluon TMDFF.

To conclude this section, we provide further discussions of our numerical estimates. First, we would like to emphasize that at the moment we only concentrate on the TMD region and we present numerical results without matching onto NLO fixed-order calculations. In other words, we have not considered the effect of the so-called Y -term which can also affect the low j_{\perp} -region, as advocated recently in [64, 65]. Second, in the TMD region, the non-perturbative parts of the quark TMDFFs have large uncertainties as they have only been constrained from SIDIS data so far, while the gluon TMDFF has not been extracted at all. Third, so far we did not take into account the effect of non-global logarithms (NGLs) [66, 67]. They first arise at next-to-next-to leading order due to the hierarchies

caused by different constraints in different phase space regions, and affect our results at the current logarithmic accuracy we are considering. The factorization and resummation of NGLs have been studied recently in great detail, see for example Refs. [68–74]. We expect to obtain significant improvements of our results in the comparison with the experimental data once all these additional factors are taken into account. A dedicated study including all additional effects will be presented in a forthcoming publication.

4 Conclusions

In this work, we have studied the hadron transverse momentum j_{\perp} -distribution within jets, where j_{\perp} is defined with respect to the standard jet axis. We set up a factorization formalism that allows for systematic studies of this distribution. As a first step we calculated all the components of the factorization theorem to NLO, and we further resummed all the associated large logarithms $\ln R$ and $\ln(p_T R/j_{\perp})$. We demonstrated the universality of the TMDFFs that arise for this jet substructure observable and the traditional TMDFFs probed in SIDIS and electron-positron annihilation. We further showed that the hadron distribution within jets produced in pp collisions provides a unique opportunity to study the TMDFFs, especially the gluon TMDFF. For SIDIS and electron-positron annihilation, the gluon TMDFF is usually difficult to access. More specifically, we showed that different than for SIDIS, the j_{\perp} spectrum within jets only depends on TMDFFs. There is no dependence on TMDPDFs which allows for a more direct extraction of TMDFFs. Furthermore, we found that at LHC energies we are able to control the sensitivity to different TMDFFs by selecting different values of the jet p_T . We observed that the low jet p_T region is the ideal region to extract the gluon TMDFF. For large jet p_T , the region away from the peak of the j_{\perp} -spectrum can also be sensitive to the gluon TMDFF.

In the future, several extensions of this work are possible. For instance, in order to extend our calculations to the region where $j_{\perp} \sim p_T R$, we need to match the resummed result onto fixed order calculations. Such a matching calculation includes the full NLO corrections to this spectrum which may also affect the TMD region. In addition, it will be important to study the numerical impact of NGLs. Besides improvements of the perturbative calculation, a more careful study of the non-perturbative Sudakov evolution will be necessary to determine whether the agreement with the data in the region $j_{\perp} < 1$ GeV can be improved. Also given the relative simple structure of the TMDFFs and the soft functions considered here, a next-to-next-to leading order calculation is possible which will further push forward the accuracy of the theoretical predictions. In this work, we only considered the phenomenology of pp collisions but the formalism developed here is also directly applicable to ep scattering relevant for a future Electron-Ion Collider (EIC). Other phenomenological studies may include for example a global fit of TMDFFs using also data from SIDIS and electron-positron annihilation. Finally, we are also planning to extend our formalism to the polarized case which is crucial to probe the Collins function, Hyperon polarization inside jets and other types of jet substructure observables.

Acknowledgments

We thank H.-n. Li, Y. Makris, A. Metz, D. Neill, J. Qiu, I. Scimemi, I. Stewart, and W. Waalewijn for discussions and comments. This work is supported by the Department of Energy under Contract Nos. DE-AC52-06NA25396, DE-AC02-05CH11231, DE-FG02-91ER40684 and DE-AC02-06CH11357, and by the Laboratory Directed Research and Development Program of Lawrence Berkeley National Laboratory. X.L. is grateful for the hospitality of the Theoretical Division at Los Alamos National Laboratory and Kavli Institute of Theoretical Physics in Santa Barbara during the completion of this manuscript.

References

- [1] A. Altheimer et al., *Boosted objects and jet substructure at the LHC. Report of BOOST2012, held at IFIC Valencia, 23rd-27th of July 2012*, *Eur. Phys. J.* **C74** (2014), no. 3 2792, [[arXiv:1311.2708](#)].
- [2] D. Adams et al., *Towards an Understanding of the Correlations in Jet Substructure*, *Eur. Phys. J.* **C75** (2015), no. 9 409, [[arXiv:1504.00679](#)].
- [3] **ATLAS** Collaboration, G. Aad et al., *Measurement of the jet fragmentation function and transverse profile in proton-proton collisions at a center-of-mass energy of 7 TeV with the ATLAS detector*, *Eur. Phys. J.* **C71** (2011) 1795, [[arXiv:1109.5816](#)].
- [4] E. C. Aschenauer et al., *The RHIC Spin Program: Achievements and Future Opportunities*, [[arXiv:1304.0079](#)].
- [5] E.-C. Aschenauer et al., *The RHIC SPIN Program: Achievements and Future Opportunities*, [[arXiv:1501.01220](#)].
- [6] E.-C. Aschenauer et al., *The RHIC Cold QCD Plan for 2017 to 2023: A Portal to the EIC*, [[arXiv:1602.03922](#)].
- [7] F. Yuan, *Azimuthal asymmetric distribution of hadrons inside a jet at hadron collider*, *Phys. Rev. Lett.* **100** (2008) 032003, [[arXiv:0709.3272](#)].
- [8] J. C. Collins, *Fragmentation of transversely polarized quarks probed in transverse momentum distributions*, *Nucl. Phys.* **B396** (1993) 161–182, [[hep-ph/9208213](#)].
- [9] R. Bain, Y. Makris, and T. Mehen, *Transverse Momentum Dependent Fragmenting Jet Functions with Applications to Quarkonium Production*, *JHEP* **11** (2016) 144, [[arXiv:1610.06508](#)].
- [10] D. Neill, I. Scimemi, and W. J. Waalewijn, *Jet axes and universal transverse-momentum-dependent fragmentation*, *JHEP* **04** (2017) 020, [[arXiv:1612.04817](#)].
- [11] M. Procura and I. W. Stewart, *Quark Fragmentation within an Identified Jet*, *Phys. Rev.* **D81** (2010) 074009, [[arXiv:0911.4980](#)]. [Erratum: *Phys. Rev.*D83,039902(2011)].
- [12] A. Jain, M. Procura, and W. J. Waalewijn, *Parton Fragmentation within an Identified Jet at NNLL*, *JHEP* **05** (2011) 035, [[arXiv:1101.4953](#)].
- [13] F. Arleo, M. Fontannaz, J.-P. Guillet, and C. L. Nguyen, *Probing fragmentation functions from same-side hadron-jet momentum correlations in p-p collisions*, *JHEP* **04** (2014) 147, [[arXiv:1311.7356](#)].

- [14] T. Kaufmann, A. Mukherjee, and W. Vogelsang, *Hadron Fragmentation Inside Jets in Hadronic Collisions*, *Phys. Rev.* **D92** (2015), no. 5 054015, [[arXiv:1506.01415](#)].
- [15] Y.-T. Chien, Z.-B. Kang, F. Ringer, I. Vitev, and H. Xing, *Jet fragmentation functions in proton-proton collisions using soft-collinear effective theory*, *JHEP* **05** (2016) 125, [[arXiv:1512.06851](#)].
- [16] Z.-B. Kang, F. Ringer, and I. Vitev, *Jet substructure using semi-inclusive jet functions in SCET*, *JHEP* **11** (2016) 155, [[arXiv:1606.07063](#)].
- [17] C. W. Bauer, S. Fleming, and M. E. Luke, *Summing Sudakov logarithms in $B \rightarrow X(s\gamma)$ in effective field theory*, *Phys. Rev.* **D63** (2000) 014006, [[hep-ph/0005275](#)].
- [18] C. W. Bauer, S. Fleming, D. Pirjol, and I. W. Stewart, *An Effective field theory for collinear and soft gluons: Heavy to light decays*, *Phys. Rev.* **D63** (2001) 114020, [[hep-ph/0011336](#)].
- [19] C. W. Bauer and I. W. Stewart, *Invariant operators in collinear effective theory*, *Phys. Lett.* **B516** (2001) 134–142, [[hep-ph/0107001](#)].
- [20] C. W. Bauer, D. Pirjol, and I. W. Stewart, *Soft collinear factorization in effective field theory*, *Phys. Rev.* **D65** (2002) 054022, [[hep-ph/0109045](#)].
- [21] C. W. Bauer, S. Fleming, D. Pirjol, I. Z. Rothstein, and I. W. Stewart, *Hard scattering factorization from effective field theory*, *Phys. Rev.* **D66** (2002) 014017, [[hep-ph/0202088](#)].
- [22] Z.-B. Kang, F. Ringer, and I. Vitev, *The semi-inclusive jet function in SCET and small radius resummation for inclusive jet production*, *JHEP* **10** (2016) 125, [[arXiv:1606.06732](#)].
- [23] A. Mukherjee and W. Vogelsang, *Jet production in (un)polarized pp collisions: dependence on jet algorithm*, *Phys. Rev.* **D86** (2012) 094009, [[arXiv:1209.1785](#)].
- [24] Z.-B. Kang, F. Ringer, and W. J. Waalewijn, *The Energy Distribution of Subjets and the Jet Shape*, [arXiv:1705.05375](#).
- [25] A. Jain, M. Procura, and W. J. Waalewijn, *Fully-Unintegrated Parton Distribution and Fragmentation Functions at Perturbative k_T* , *JHEP* **04** (2012) 132, [[arXiv:1110.0839](#)].
- [26] J. Collins, *Foundations of perturbative QCD*. Cambridge University Press, 2013.
- [27] T. Becher, M. Neubert, L. Rothen, and D. Y. Shao, *Effective Field Theory for Jet Processes*, *Phys. Rev. Lett.* **116** (2016), no. 19 192001, [[arXiv:1508.06645](#)].
- [28] Y.-T. Chien, A. Hornig, and C. Lee, *A Soft-Collinear Mode for Jet Cross Sections in Soft Collinear Effective Theory*, [arXiv:1509.04287](#).
- [29] J.-Y. Chiu, A. Jain, D. Neill, and I. Z. Rothstein, *A Formalism for the Systematic Treatment of Rapidity Logarithms in Quantum Field Theory*, *JHEP* **05** (2012) 084, [[arXiv:1202.0814](#)].
- [30] M. G. Echevarria, A. Idilbi, Z.-B. Kang, and I. Vitev, *QCD Evolution of the Sivers Asymmetry*, *Phys. Rev.* **D89** (2014) 074013, [[arXiv:1401.5078](#)].
- [31] S. M. Aybat and T. C. Rogers, *TMD Parton Distribution and Fragmentation Functions with QCD Evolution*, *Phys. Rev.* **D83** (2011) 114042, [[arXiv:1101.5057](#)].
- [32] M. G. Echevarria, A. Idilbi, and I. Scimemi, *Factorization Theorem For Drell-Yan At Low q_T And Transverse Momentum Distributions On-The-Light-Cone*, *JHEP* **07** (2012) 002, [[arXiv:1111.4996](#)].
- [33] J. C. Collins and D. E. Soper, *Back-To-Back Jets in QCD*, *Nucl. Phys.* **B193** (1981) 381. [Erratum: *Nucl. Phys.*B213,545(1983)].

- [34] X.-d. Ji, J.-p. Ma, and F. Yuan, *QCD factorization for semi-inclusive deep-inelastic scattering at low transverse momentum*, *Phys. Rev.* **D71** (2005) 034005, [[hep-ph/0404183](#)].
- [35] X.-d. Ji, J.-P. Ma, and F. Yuan, *QCD factorization for spin-dependent cross sections in DIS and Drell-Yan processes at low transverse momentum*, *Phys. Lett.* **B597** (2004) 299–308, [[hep-ph/0405085](#)].
- [36] T. Kasemets, W. J. Waalewijn, and L. Zeune, *Calculating Soft Radiation at One Loop*, *JHEP* **03** (2016) 153, [[arXiv:1512.00857](#)].
- [37] J. C. Collins, D. E. Soper, and G. F. Sterman, *Transverse Momentum Distribution in Drell-Yan Pair and W and Z Boson Production*, *Nucl. Phys.* **B250** (1985) 199–224.
- [38] M. G. Echevarria, A. Idilbi, A. Schafer, and I. Scimemi, *Model-Independent Evolution of Transverse Momentum Dependent Distribution Functions (TMDs) at NNLL*, *Eur. Phys. J.* **C73** (2013), no. 12 2636, [[arXiv:1208.1281](#)].
- [39] A. Kulesza, G. F. Sterman, and W. Vogelsang, *Joint resummation in electroweak boson production*, *Phys. Rev.* **D66** (2002) 014011, [[hep-ph/0202251](#)].
- [40] J.-w. Qiu and X.-f. Zhang, *Role of the nonperturbative input in QCD resummed Drell-Yan Q_T distributions*, *Phys. Rev.* **D63** (2001) 114011, [[hep-ph/0012348](#)].
- [41] S. Catani, D. de Florian, G. Ferrera, and M. Grazzini, *Vector boson production at hadron colliders: transverse-momentum resummation and leptonic decay*, *JHEP* **12** (2015) 047, [[arXiv:1507.06937](#)].
- [42] M. A. Ebert and F. J. Tackmann, *Resummation of Transverse Momentum Distributions in Distribution Space*, *JHEP* **02** (2017) 110, [[arXiv:1611.08610](#)].
- [43] P. F. Monni, E. Re, and P. Torrielli, *Higgs Transverse-Momentum Resummation in Direct Space*, *Phys. Rev. Lett.* **116** (2016), no. 24 242001, [[arXiv:1604.02191](#)].
- [44] R. K. Ellis and J. C. Sexton, *QCD Radiative Corrections to Parton Parton Scattering*, *Nucl. Phys.* **B269** (1986) 445–484.
- [45] F. Aversa, P. Chiappetta, M. Greco, and J. P. Guillet, *QCD Corrections to Parton-Parton Scattering Processes*, *Nucl. Phys.* **B327** (1989) 105.
- [46] M. Dasgupta, F. Dreyer, G. P. Salam, and G. Soyez, *Small-radius jets to all orders in QCD*, *JHEP* **04** (2015) 039, [[arXiv:1411.5182](#)].
- [47] L. Dai, C. Kim, and A. K. Leibovich, *Fragmentation of a Jet with Small Radius*, *Phys. Rev.* **D94** (2016), no. 11 114023, [[arXiv:1606.07411](#)].
- [48] S. Dulat, T.-J. Hou, J. Gao, M. Guzzi, J. Huston, P. Nadolsky, J. Pumplin, C. Schmidt, D. Stump, and C. P. Yuan, *New parton distribution functions from a global analysis of quantum chromodynamics*, *Phys. Rev.* **D93** (2016), no. 3 033006, [[arXiv:1506.07443](#)].
- [49] B. Jager, A. Schafer, M. Stratmann, and W. Vogelsang, *Next-to-leading order QCD corrections to high $p(T)$ pion production in longitudinally polarized pp collisions*, *Phys. Rev.* **D67** (2003) 054005, [[hep-ph/0211007](#)].
- [50] **HERMES** Collaboration, A. Airapetian et al., *Multiplicities of charged pions and kaons from semi-inclusive deep-inelastic scattering by the proton and the deuteron*, *Phys. Rev.* **D87** (2013) 074029, [[arXiv:1212.5407](#)].
- [51] **COMPASS** Collaboration, C. Adolph et al., *Hadron Transverse Momentum Distributions*

- in Muon Deep Inelastic Scattering at 160 GeV/c*, *Eur. Phys. J.* **C73** (2013), no. 8 2531, [[arXiv:1305.7317](#)]. [Erratum: *Eur. Phys. J.* C75,no.2,94(2015)].
- [52] M. Boglione, J. Collins, L. Gamberg, J. O. Gonzalez-Hernandez, T. C. Rogers, and N. Sato, *Kinematics of Current Region Fragmentation in Semi-Inclusive Deeply Inelastic Scattering*, *Phys. Lett.* **B766** (2017) 245–253, [[arXiv:1611.10329](#)].
- [53] Z.-B. Kang, A. Prokudin, P. Sun, and F. Yuan, *Extraction of Quark Transversity Distribution and Collins Fragmentation Functions with QCD Evolution*, *Phys. Rev.* **D93** (2016), no. 1 014009, [[arXiv:1505.05589](#)].
- [54] P. Sun, J. Isaacson, C. P. Yuan, and F. Yuan, *Universal Non-perturbative Functions for SIDIS and Drell-Yan Processes*, [arXiv:1406.3073](#).
- [55] A. Bacchetta, F. Delcarro, C. Pisano, M. Radici, and A. Signori, *Extraction of partonic transverse momentum distributions from semi-inclusive deep-inelastic scattering, Drell-Yan and Z-boson production*, [arXiv:1703.10157](#).
- [56] C. Balazs, E. L. Berger, S. Mrenna, and C. P. Yuan, *Photon pair production with soft gluon resummation in hadronic interactions*, *Phys. Rev.* **D57** (1998) 6934–6947, [[hep-ph/9712471](#)].
- [57] C. Balazs and C. P. Yuan, *Higgs boson production at the LHC with soft gluon effects*, *Phys. Lett.* **B478** (2000) 192–198, [[hep-ph/0001103](#)].
- [58] C. Balazs, E. L. Berger, P. M. Nadolsky, and C. P. Yuan, *Calculation of prompt diphoton production cross-sections at Tevatron and LHC energies*, *Phys. Rev.* **D76** (2007) 013009, [[arXiv:0704.0001](#)].
- [59] D. de Florian, R. Sassot, and M. Stratmann, *Global analysis of fragmentation functions for protons and charged hadrons*, *Phys. Rev.* **D76** (2007) 074033, [[arXiv:0707.1506](#)].
- [60] A. Vogt, *Efficient evolution of unpolarized and polarized parton distributions with QCD-PEGASUS*, *Comput. Phys. Commun.* **170** (2005) 65–92, [[hep-ph/0408244](#)].
- [61] D. P. Anderle, F. Ringer, and M. Stratmann, *Fragmentation Functions at Next-to-Next-to-Leading Order Accuracy*, *Phys. Rev.* **D92** (2015), no. 11 114017, [[arXiv:1510.05845](#)].
- [62] G. T. Bodwin, H. S. Chung, U.-R. Kim, and J. Lee, *Fragmentation contributions to J/ψ production at the Tevatron and the LHC*, *Phys. Rev. Lett.* **113** (2014), no. 2 022001, [[arXiv:1403.3612](#)].
- [63] D. de Florian, R. Sassot, M. Epele, R. J. Hernandez-Pinto, and M. Stratmann, *Parton-to-Pion Fragmentation Reloaded*, *Phys. Rev.* **D91** (2015), no. 1 014035, [[arXiv:1410.6027](#)].
- [64] J. Collins, L. Gamberg, A. Prokudin, T. C. Rogers, N. Sato, and B. Wang, *Relating Transverse Momentum Dependent and Collinear Factorization Theorems in a Generalized Formalism*, *Phys. Rev.* **D94** (2016), no. 3 034014, [[arXiv:1605.00671](#)].
- [65] M. Boglione, J. O. Gonzalez Hernandez, S. Melis, and A. Prokudin, *A study on the interplay between perturbative QCD and CSS/TMD formalism in SIDIS processes*, *JHEP* **02** (2015) 095, [[arXiv:1412.1383](#)].
- [66] M. Dasgupta and G. Salam, *Resummation of nonglobal QCD observables*, *Phys. Lett.* **B512** (2001) 323–330, [[hep-ph/0104277](#)].

- [67] A. Banfi, G. Marchesini, and G. Smye, *Away from jet energy flow*, *JHEP* **0208** (2002) 006, [[hep-ph/0206076](#)].
- [68] M. Dasgupta, K. Khelifa-Kerfa, S. Marzani, and M. Spannowsky, *On jet mass distributions in Z +jet and dijet processes at the LHC*, *JHEP* **1210** (2012) 126, [[arXiv:1207.1640](#)].
- [69] A. J. Larkoski, I. Moulton, and D. Neill, *Non-Global Logarithms, Factorization, and the Soft Substructure of Jets*, *JHEP* **09** (2015) 143, [[arXiv:1501.04596](#)].
- [70] A. J. Larkoski, I. Moulton, and D. Neill, *The Analytic Structure of Non-Global Logarithms: Convergence of the Dressed Gluon Expansion*, *JHEP* **11** (2016) 089, [[arXiv:1609.04011](#)].
- [71] D. Neill, *The Asymptotic Form of Non-Global Logarithms, Black Disc Saturation, and Gluonic Deserts*, *JHEP* **01** (2017) 109, [[arXiv:1610.02031](#)].
- [72] T. Becher, M. Neubert, L. Rothen, and D. Y. Shao, *Factorization and Resummation for Jet Processes*, *JHEP* **11** (2016) 019, [[arXiv:1605.02737](#)].
- [73] S. Caron-Huot, *Resummation of non-global logarithms and the BFKL equation*, [[arXiv:1501.03754](#)].
- [74] Y. Hagiwara, Y. Hatta, and T. Ueda, *Hemisphere jet mass distribution at finite N_c* , *Phys. Lett.* **B756** (2016) 254–258, [[arXiv:1507.07641](#)].